UNIVERSITY OF

MARYLAND

THE INSTITUTE FOR FLUID DYNAMICS

and

APPLIED MATHEMATICS

Technical Note BN-627 November 1969

NUMERICAL SOLUTION OF LAMINAR JET MIXING WITH AND WITHOUT FREE STREAM*

by

S. I. Pai and T. Y. Hsieh

University of Maryland
College Park, Maryland

*This research was supported in part by the United States Army Material Command Harry Diamond Laboratories under Contract No. DAAG39-69-C-0036. The computer time for this report was supported by National Aeronautics and Space Administration Grant NSG-398 to the Computer Science Center of the University of Maryland.

TABLE OF CONTENTS

ABSTRACT

In Part A, systematic numerical solutions of two dimensional and axisymmetrical laminar jet of an incompressible fluid with and without free stream have been obtained. The exact numerical solutions have been checked with experimental results and similarity solutions for the case without free stream. At far downstream, the numerical solutions approach the values of similarity solution. The numerical solutions give better agreement with experimental data than the similarity solutions. In general, it shows that the boundary layer equation is a good approximation of laminar jet problem provided that the Reynolds number at nozzle exit is not too low. With free stream, the numerical solutions agree with linearized analytic solution if the jet excess velocity is small in comparison with the free stream velocity. The non-linear effects are to decrease the rate of decrease of central velocity of the jet and to broaden the spread of the jet.

In Part B, an approximate numerical solution for three dimensional laminar jet is proposed. The accuracy of the method has been determined from the exact solutions of the two limiting cases of three dimensional jets, i.e., two dimensional and axisymmetric case of Part A. It was found that this approximate method may give good results for the axial velocity distribution and the spread of three dimensional jet.

SYMBOLS

a	Radius of circular exit
b, $\bar{b}$	Half-width of jet with and without cross flow respectively
c_2, c_r	Momentum coefficient for two-dimensional and axisymmetric jet respectively
c_u	Correction factor for central excess velocity
D	Half-width of the shorter side of rectangular jet exit
h	Spacing in x direction
J_o, J_1	Bessel function of zeroth and first order of the first kind respectively
k	Spacing in z direction
L	Aspect ratio of rectangular jet exit
M_2, M_r	Total momentum of two dimensional and axisymmetric jet respectively
p	Spacing in y direction
R_e, $\bar{R}_e$	Reynolds number defined $\frac{U_j^* D}{\nu}$ and $\frac{\bar{U}^* a}{\nu}$ respectively
u^*, v^*, w^*	Excess velocity components along x^*, y^* and z^* direction respectively
u, v, w	Non-dimensional excess velocity components defined by u^*/U_j^*, $R_e v^*/U_j^*$ and $R_e w^*/U_j^*$ respectively

SYMBOLS

u_m, $\bar{u}_m$	Non-dimensional maximum excess velocity over a station with and without cross flow respectively
u_i	Non-dimensional excess velocity distribution at jet exit
U_o^*	Uniform velocity of moving stream
U_o	Non-dimensional uniform velocity of moving stream (U_o^*/U_j^*)
U_j^*	Excess velocity at the center of jet exit
$\bar{U}^*$	Mean excess velocity at jet exit
x^*, y^*, z^*	Axis of Cartesian coordinate
x, y, z	Non-dimensional distance defined by x^*/R_eD , y^*/D and z^*/D respectively
ξ	Non-dimensional parameter defined by Eq. (10)
δ	A constant
ν	Kinematic viscosity of fluid
ρ	Density of fluid

Subscript:

o	Axisymmetrical jet
∞	Two-dimensional jet
L	Three dimensional jet with aspect ratio L

Superscript:

-	Without cross flow

I. INTRODUCTION

In most of the theoretical investigations of laminar jet mixing, only the similar solutions[1,2] or the solutions of linearized equations[1,3] have been discussed. Very little general solutions of laminar jet mixing have been obtained. In the first part of this report, we study numerical solutions of two dimensional as well as axisymmetric laminar jet mixing of an incompressible fluid with and without free stream systemmatically. We are especially interested in the non-similar solutions of these problems. The influence of initial velocity profiles and the effect of non-linearity will be analyzed. The results of our numerical solutions will be compared with the well known similar solution (without free stream) and linearized solution (with free stream[3]).

In the second part of this report, numerical solutions of a three dimensional laminar jet mixing have been studied. In our preliminary attempt of solving the complete non-linear equation of a three dimensional jet mixing by computer, the numerical calculation was very unstable and so far no satisfactory results were obtained. Since we have satisfactory solutions for two dimensional and axisymmetrical laminar jet mixing in Part I, we try to find some approximation in numerical solution in the three dimensional case from the results of our two dimensional and axisymmetrical cases. We find that the two dimensional (aspect ratio is infinite) and the axisymmetrical case (aspect ratio is unity) represent two limiting cases of three dimensional laminar jet mixing from a rectangular nozzle. Hence in

general, the results of three dimensional jet mixing lie between those of two dimensional and axisymmetric cases. From the results of two dimensional and axisymmetric jets, we found that the axial velocity distributions may be obtained with sufficient accuracy by neglecting the cross-velocity effects. Hence we use similar approximation by neglecting the cross-velocity in solving the axial velocity distribution of three dimensional jet mixing, which is the most important quantity in practical application of jet mixing problems. We also discuss the accuracy of this approximate method and the improvement of the results from our experience of the exact results of two dimensional and axisymmetric cases. Numerical solutions of axial component of three dimensional jet without free stream from rectangular nozzle of aspect ratios 1, 2 and 4 have been obtained.

PART A. TWO DIMENSIONAL AND AXISYMMETRICAL JET

II. FUNDAMENTAL EQUATIONS

The fundamental equations for a steady two dimensional or an axisymmetrical laminar jet mixing of an incompressible fluid are[1,2]

$$\frac{\partial u^*}{\partial x^*} + \frac{\partial v^*}{\partial y^*} + \delta \frac{v^*}{y^*} = 0 \tag{1}$$

$$(U_o^* + u^*) \frac{\partial u^*}{\partial x^*} + v^* \frac{\partial u^*}{\partial y^*} = \frac{\nu}{y^{*\delta}} \frac{\partial}{\partial y} \left(y^{*\delta} \frac{\partial u^*}{\partial y^*} \right) \tag{2}$$

where u^* and v^* are respectively the excess axial (x^* - wise) velocity over the free stream U_o and the transverse or radial (y^* - wise) velocity component; $\delta = 0$ for two dimensional case and $\delta = 1$ for axisymmetrical case; U_o^* is a constant velocity of free stream and ν is the coefficient of kinematical viscosity of the fluid which is assumed to be constant in this report. The pressure in the flow field is assumed to be constant in this report. When the surrounding stream is at rest, U_o^* is zero.

The initial and boundary conditions of both two dimensional and axisymmetrical laminar jet are:

$$\begin{aligned} x^* = 0 \ ; \quad & u^* = u_1^*(0, y^*) \\ x^* > 0 \ ; \quad & v^* = 0 \quad \text{at} \quad y^* = 0 \\ & u^* = 0 \quad \text{at} \quad y^* \to \infty \ . \end{aligned} \tag{3}$$

We solve Eqs. (1) and (2) with the initial and boundary conditions (3) where $u_i(0,y^*)$ is a given function of y^*. In the numerical calculation, it is convenient to introduce the following non-dimensional quantities.

$$u = \frac{u^*}{U_j^*} \quad , \quad v = R_e \cdot \frac{v^*}{U_j^*} \quad , \quad U_o = \frac{U_o^*}{U_j^*} \quad , \quad u_i = \frac{u_i^*}{U_j^*} \tag{4}$$

$$x = \frac{x^*}{D\,R_e} \quad , \quad y = \frac{y^*}{D} \quad , \quad R_e = \frac{U_j^* D}{\nu}$$

where U_j^* is the value of u^* at the center line of the exit of the nozzle, D is the half width or the radius of the jet exit and R_e is the Reynolds number of the present problem. In terms of the non-dimensional quantities of Eq. (4), the fundamental equations (1) and (2) are independent of the Reynolds number R_e and are as follows:

$$\frac{\partial u}{\partial x} + \frac{\partial v}{\partial y} + \delta \frac{v}{y} = 0 \tag{5}$$

$$(U_o + u) \frac{\partial u}{\partial x} + \frac{\partial v}{\partial y} = \frac{1}{y^\delta} \frac{\partial}{\partial y} \left(y^\delta \frac{\partial u}{\partial y}\right) \tag{6}$$

It should be noted that at the axis of the axisymmetrical case $\frac{1}{y} \frac{\partial u}{\partial y} = \frac{\partial^2 u}{\partial y^2}$ and $\frac{v}{y} = \frac{\partial v}{\partial y}$.

We are going to solve Eqs. (5) and (6) for the following three different initial velocity profiles:

(a) Rectangular Profile:

$$u_i = 1 \qquad y \leq 1$$
$$u_i = 0 \qquad y > 1 \tag{7}$$

(b) Parabolic Profile:

$$u_i = (1-y^2) \qquad y \leq 1$$
$$u_i = 0 \qquad y > 0 \tag{8}$$

(c) Triangular Profile:

$$u_i = 1-y \qquad y \leq 1$$
$$u_i = 0 \qquad y > 0 \tag{9}$$

III. SIMILARITY SOLUTIONS OF TWO-DIMENSIONAL AND AXISYMMETRICAL JET

Similarity solutions occur for the case without free stream ($U_o^* = 0$) only. For two dimensional jet, Bickley gave the closed form similarity solutions as follows:[1]

$$u^* = 0.4543\left(\frac{M_2^2}{\rho^2 \nu x^*}\right)^{1/3} \tanh \xi$$

$$v^* = 0.5503\left(\frac{M_2 \nu}{\rho x^{*2}}\right)^{1/3} [2\xi(1-\tanh^2 \xi) - \tanh \xi] \tag{10}$$

$$\xi = 0.2752\left(\frac{M_2}{\rho \nu^2}\right)^{1/3} \frac{y^*}{x^{*2/3}}$$

where M_2 is the total momentum across a section of the two dimensional jet.

For axisymmetrical jet, Schlichting gave the closed form similarity solution[1] as:

$$u^* = \frac{3}{8\pi} \frac{M_r}{\rho \nu x^*} \frac{1}{(1 + 1/4\xi^2)^2}$$

$$v^* = \frac{1}{4}\sqrt{\frac{3}{\pi}} \frac{M_r^{1/2}}{x^* \rho^{1/2}} \frac{\xi - 1/4\xi^3}{(1 + 1/4\xi^2)^2} \tag{11}$$

$$\xi = \sqrt{\frac{3}{16\pi}} \frac{M_r^{1/2}}{\nu \rho^{1/2}} \frac{y^*}{x^*}$$

where M_r is the momentum across a section of the axisymmetrical jet.

Let

$$M_2 = C_2 \rho U_j^{*2} D \tag{12}$$

then $C_2 = 2, \frac{16}{15}$ and $2/3$ respectively for rectangular, parabolic and triangular initial velocity distributions. Similarly, let

$$M_r = C_r \rho \pi D^2 U_j^{*2} \tag{13}$$

then $C_r = 1$ and $1/3$ respectively for rectangular and parabolic initial velocity distribution.

Hence Eqs. (10) and (11) may be written, in terms of non-dimensional forms, as follows:

For two dimensional jet

$$u = 0.4543\left(\frac{C_2^2}{x}\right)^{1/3}(1 - \tanh \xi)$$

$$v = 0.5503\left(\frac{C_2}{x^2}\right)^{1/3}[2\xi(1-\tanh^2\xi) - \tanh \xi] \qquad (14)$$

$$\xi = 0.2752\ C_2^{1/3}\ y/x^{2/3} \quad .$$

For axi-symmetrical jet

$$u = \frac{3}{8} \cdot \frac{C_r}{x} \cdot \frac{1}{(1 + \frac{1}{4}\xi^2)^2}$$

$$v = \frac{\sqrt{3}}{4} \frac{C_r^{1/2}}{x} \cdot \frac{\xi - \frac{1}{4}\xi^3}{(1 + \frac{1}{4}\xi^2)^2} \qquad (15)$$

$$\xi = \sqrt{\frac{3}{16}}\ C_r^{1/2}\ y/x$$

IV. LINEARIZED SOLUTIONS WITH UNIFORM FREE STREAM VELOCITY U_o.

When $U_o^* >> U_j^*$, the fundamental equations of laminar jet mixing may be linearized. Pai[1] gave the following linearized solutions;

For two dimensional jet

$$u = \frac{1}{2}[\mathrm{erf}(\frac{1-y}{2\sqrt{x_o}}) + \mathrm{erf}(\frac{1+y}{2\sqrt{x_o}})] \qquad (16)$$

and for axisymmetrical jet

$$u = \int_0^\infty e^{-\lambda^2 x_o} J_o(\lambda y)\, J_1(\lambda)\, d\lambda \qquad (17)$$

where $x_o = x/U_o$. Eqs. (16) and (17) are for the rectangular initial velocity profiles only.

V. NUMERICAL SOLUTIONS OF TWO DIMENSIONAL AND AXISYMMETRICAL JETS WITH AND WITHOUT UNIFORM FREE STREAM VELOCITY.

The numerical calculation has been carried out on the Univac 1108 computer of the Computer Science Center of the University of Maryland. An implicit finite difference method as described in Reference 4 was used for the present calculation. We write

$$\frac{\partial Q}{\partial x} = \frac{1}{h}(Q_n - Q_{n-1}) \qquad \text{forward difference}$$

$$\frac{\partial Q}{\partial y} = \frac{1}{2p}(Q_{m+1} - Q_{m-1}) \qquad \text{central difference}$$

$$\frac{\partial^2 Q}{\partial y^2} = \frac{1}{p^2}(Q_{m+1} - 2Q_m + Q_{m-1}) \qquad \text{central difference}$$

where n refers to station in x-direction and m , that in y-direction; Q denotes any quantity under operation, $h = \Delta x$ and $p = \Delta y$ denote respectively

the spacing in x and y directions. Substituting the finite difference representations in Eqs. (5) and (6), we have

$$\{1 + [v - \frac{\delta}{(m-1)p}]\frac{p}{2}\} u_{n,m-1} - (2 + \frac{up^2}{h}) u_{n,m} +$$

$$+ \{1 - [v - \frac{\delta}{(m-1)p}]\frac{p}{2}\} u_{n,m+1} = - \frac{u\, u_{n-1,m}\, p^2}{h} \qquad (18)$$

and

$$v = - \frac{1}{y^\delta} \int_0^y (\frac{\partial u}{\partial x})\, y^\delta \, dy \qquad (19)$$

where u and v appear in the coefficient are considered to be the known values at station (n,m). The trapazoidal rule was used for the integration of v. In practical calculation, the previous known values of $u_{n-1,m}$ and $v_{n-1,m}$ were first used in the coefficients for u and v to obtain $u_{n,m}$ and $v_{n,m}$. Then iteration was carried out by replacing the new $u_{n,m}$ and $v_{n,m}$ in the coefficient until a satisfactory result for $u_{n,m}$ and $v_{n,m}$ was obtained. Therefore, the u and v thus obtained in a station (n,m) satisfy the fundamental equations and boundary conditions exactly. The method of solving the simultaneous equations for $u_{n,m}$ is given in Appendix I.

In principle, the boundary of the free jet is infinite. However, in the actual computation, it was found that the boundary could be set at 20D where D is the half width of the nozzle opening for good results in

the range presented in this report. In the initial stations, the value of h was set at 0.001 and as the computation proceeds downstream, the value of h is increased. The values of h used in this report are between 0.001 to 0.1 for two-dimensional jet and between 0.001 to 0.05 for axisymmetrical jet. Lateral spacing p was always kept at a value of 0.005. A test for $p = 0.1$ does not change the results significantly.

VI. RESULTS AND DISCUSSION

In jet mixing problems, we are interested in the decrease of maximum axial velocity downstream, the velocity profiles of both axial u and transverse v velocity component and the half jet width which shows the spread of the jet. The numerical results for these quantities are given below:

(a) Variation of maximum axial velocity. The non-dimensional maximum axial velocities, $u_m = u_m^*/U_j^*$ which occurs on the jet axis, are plotted as a function of non-dimensional axial distance x with rectangular initial velocity profile with various free stream velocity u_o for two dimensional jet in Fig. 1; while the correspondong curves for axisymmetrical jet in Fig. 2. It should be noted that the non-dimensional distances for cases with (x_o) and without (x) moving stream are different. For the cases with free stream, $(U_o = 0)$ three cases for $U_o = 1/2$, 1 and 10 were calculated. It is interesting to see that the numerical solution approaches the linearized solution (16) or (17) as U_o increases. This

justifies both the correctness of the linearized theory and the numerical solution.

When $U_o = 0$, the numerical solution should be compared with the similarity solution (14) or (15). These comparisons are shown in Figures 3 and 4. In Figure 3, two dimensional jets with three different initial velocity profiles (rectangular, parabolic and triangular) are compared with corresponding similarity solutions ($C_r = 2$, $16/15$ and $2/3$). In Figure 4, axisymmetric jets with two different initial velocity profiles (rectangular and parabolic) are compared with corresponding similarity solution ($C_r = 1$ and $1/3$). From both Figures 3 and 4, it is seen that in each case the similarity solution approaches the corresponding numerical solution at far downstream as expected since it is well known that similarity solution is only good at far downstream.

There are a few experimental results available for laminar two dimensional[5,6] and axisymmetrical jet.[7] These experimental data are also plotted in Figures 3 and 4.

For two dimensional laminar jet, Reference 5 gives experimental data for four different Reynolds numbers. The initial velocity profiles correspond to the parabolic distribution because it is supposed to be fully developed velocity profile from a two dimensional channel flow. We found that the agreement of experimental data with curve of parabolic initial velocity distribution is fairly well for $\overline{R}_e = 4DU_j^*/3\nu = 68$ and 31 while for $\overline{R}_e = 240$, the data approaches the values with rectangular initial velocity profile and for $\overline{R}_e = 15$, the data points are too low.

Since no initial profiles were given, we suspected that for $\bar{R}_e = 240$, the initial profile in the experiment might not reach the fully developed stage but still close to entrance rectangular profile. For $\bar{R}_e = 15$, the velocity of the jet is so low that boundary layer approximations might not be valid. From the data $\bar{R}_e = 31$ and 68 as well as the data of reference 6, $\bar{R}_e = 31.5$, the correlation between experimental and numerical results are excellent. Since in the experimental data momentum lost across the section were shown, we have to make the proper correction in comparison of the experimental data to numerical solution as follows:

$$\frac{U_j^*}{U_{j0}^*} = \frac{M_2}{M_{20}} \tag{20}$$

where subscript 0 denotes the original value at exit and M_2 is the measured momentum at downstream and U_j^* is the corrected value at exit to be used for downstream station.

In Figure 4, the experimental data of Reference 7 indicate a shift of origin of the axisymmetrical jet of $x_s = x_s^*/R_e D = 0.225$ for rectangular initial velocity distribution (a maximum value from experimental data) and $x_s = x_s^*/R_e D = 0.1$ for parabolic initial velocity distribution (an average value of experimental data. Note in Reference 7, $x_s^* = 0.15(\frac{\bar{U}^* a}{\nu})$ $= 0.1(\frac{u_j^* a}{\nu})$, $\bar{u}^* = \frac{2}{3} u_j^*$) . With the shift of origin, it is seen that the experimental data agrees extremely well with numerical solution for parabolic initial velocity distribution while it is fairly well for rectangular initial distribution. According to numerical result, x_s for the later should be 0.3 to give best agreement.

From the comparison with experimental data, it shows the validity of the boundary layer approximation for laminar two dimensional and axisymmetrical jet when the Reynolds number is not too low. Numerical solution provides the overall information of the whole flow field including those near the exit of the nozzle while similarity solution is good only far downstream.

(b) Axial velocity profile u. The axial velocities u vs. the transverse coordinate y at various value of moving stream velocity U_o are plotted in Figure 5 for two dimensional jet and in Figure 6 for axisymmetrical jet. For all the cases, the initial velocity profiles are rectangular. These velocity distributions approach to the form of linearized solution when U_o is much larger than unity.

When $U_o = 0$, we compare the numerical solution with similar solutions of Eq. (14) or (15). To compare the axial velocity profile, we plot u/u_m at constant ξ but different x in Figure 7. For similar solution, u/u_m is a constant at constant ξ but for numerical solution, u/u_m depends on both ξ and x. However as x increases, we find in Figure 7 that the numerical solution approaches to the similar solution. In Figures 8 and 9, the numerical solutions with two different initial velocity profiles are compared with the corresponding similar solutions for two dimensional and axisymmetrical jet respectively. In general, the similar solution agrees better with parabolic initial velocity distribution than with rectangular one. In all cases, the numerical solution gives broader profile near the axis of the jet than the similar solution. This fact gives better agreement of numerical solution with

experimental data than the similar solution.

(c) Transverse velocity profile v . When $U_o \neq 0$, typical v - component velocity profiles at $x = 0.1$ and $U_o = 1/2$, 1, and 10 for two dimensional jet and axisymmetrical jet are shown in Figure 10. When $U_o >> 1$, the v - velocity component is indeed very small and can be neglected.

When $U_o = 0$, Figures 11 and 12 show respectively the v - component at various x - station and for different initial velocity profiles for two dimensional and axisymmetrical jet. The corresponding similar solution is also plotted in the same figure. For rectangular initial profiles, the agreement between numerical and similar solutions becomes better as x_o increases. For parabolic initial velocity distribution, the agreement is almost perfect for $x > 0.2$.

(d) Half width of jet. Figure 13 shows the spread of half width $b = b^*/D$ where $u/u_m = 1/2$ as a function of axial distance x or x_o for two dimensional and axisymmetrical jet. Experimental data of reference 7 with proper correction as discussed above and also data of references 5 and 6 are also given in Figure 13. The experimental data show a broader jet than the theoretical prediction by about 10% for two dimensional jet and 2.5% for axisymmetrical jet. The experimental line for rectangular initial profile of axisymmetrical jet should not be compared directly with the numerical solution because there is a difference in the maximum jet velocity in these two cases because of the momentum loss in the experimental data. Should $x_s = 0.3$ be used as recommended

in section (a), then the experimental data is again broader than theoretical prediction as described in Reference 7. The spread of half width of linearized solution is also shown in Figure 13.

PART B. THREE DIMENSIONAL JET

VII. FUNDAMENTAL EQUATIONS

The non-dimensional fundamental equations for a steady three dimensional laminar jet mixing of an incompressible fluid[3] are as follows*:

$$\left.\begin{aligned} (U_o + u)\frac{\partial u}{\partial x} + v\frac{\partial u}{\partial y} + w\frac{\partial u}{\partial z} &= \frac{\partial^2 u}{\partial y^2} + \frac{\partial^2 u}{\partial z^2} \\ (U_o + u)\frac{\partial w}{\partial x} + v\frac{\partial w}{\partial y} + w\frac{\partial w}{\partial z} &= \frac{\partial^2 w}{\partial y^2} + \frac{\partial^2 w}{\partial z^2} \\ \frac{\partial u}{\partial x} + \frac{\partial v}{\partial y} + \frac{\partial w}{\partial z} &= 0 \end{aligned}\right\} \qquad (21)$$

The non-dimensional quantities are the same as those of part A with $w = R_e \frac{w^*}{U_j^*}$ and $z = z^*/D$.

The intial and boundary conditions for Eq. (21) are:

---

*From a discussion of Professor Isaac Greber, the z-momentum equation should be replaced by a vorticity equation. Since this change will not affect the results of the present report, we shall look into this problem in our future research program.

$$
\left.
\begin{aligned}
&x = 0: \quad u_i = 1 \quad \text{for} \quad y \leq 1 \quad \text{and} \quad z \leq 1 \\
&\qquad\quad u_i = 0 \quad \text{for} \quad y > 1\,, \quad z > L \\
&x > 0: \quad v = \frac{\partial w}{\partial y} = 0 \quad \text{along} \quad z = 0 \\
&\qquad\quad w = \frac{\partial v}{\partial z} = 0 \quad \text{along} \quad y = 0 \\
&\qquad\quad u = \frac{\partial w}{\partial z} = \frac{\partial v}{\partial y} = 0 \quad \text{at} \quad y \to \infty\,, \quad z \to \infty\,.
\end{aligned}
\right\} \qquad (22)
$$

where L is the aspect ratio of rectangular exit. In this report, we shall consider the case $U_o = 0$ only.

VIII. NUMERICAL METHOD

The alternating direction implicit finite difference method described in reference 8 seems most suitable for the present problem. The basic principle is the same as that described in section V. However, the progress in x - direction is completed in two steps. First we treat one direction (e.g., z - direction) as unchanged and then we treat the other direction (e.g., y - direction) as unchanged. Therefore, in each step, the problem is essentially the same as two dimensional one. This method was proved to be unconditionally stable for linear three dimensional equation.

Applying forward difference in x - direction and central difference in y and z directions as described in section V, the x-momentum equation in Eq. (21) can be written in finite different form as follows:

$$-\left(\frac{wp}{2}+1\right)u_{\ell-\frac{1}{2},m,n-1}+\left(\frac{up^2}{h}+2\right)u_{\ell-\frac{1}{2},m,n}+\left(\frac{pw}{2}-1\right)u_{\ell-\frac{1}{2},m,n+1}=$$

$$=\frac{p^2}{k^2}\left[\left(1-\frac{kv}{2}\right)u_{\ell-1,m+1,n}-\left(2-\frac{k^2u}{h}\right)u_{\ell-1,m,n}+\left(1+\frac{vk}{2}\right)u_{\ell-1,m-1,n}\right] \qquad (23a)$$

$$-\left(\frac{kv}{2}+1\right)u_{\ell,m-1,n}+\left(\frac{k^2u}{h}+2\right)u_{\ell,m,n}+\left(\frac{kv}{2}-1\right)u_{\ell,m+1,n}=$$

$$=\frac{k^2}{p^2}\left[\left(1-\frac{wp}{2}\right)u_{\ell-\frac{1}{2},m,n+1}-\left(2-\frac{up^2}{h}\right)u_{\ell-\frac{1}{2},m,n}+\left(1+\frac{wp}{2}\right)u_{\ell-\frac{1}{2},m,n+1}\right] \qquad (23b)$$

where h is the half spacing in the x - direction, and p, k are respectively the y- and z-spacing. The subscripts ℓ, m, and n represent the position of grid point in x, y and z direction respectively.

The finite difference forms for the z-momentum equation in Eq. (21) are the same as Eqs. (23a) and (23b). They will not be written down. Because we find that the numerical solutions for these complete non-linear three dimensional equations (23), etc. are highly unstable. We have to use some approximation described in the next section to obtain some useful results of the present problem in which the z - momentum equation may be neglected.

IX. APPROXIMATE NUMERICAL SOLUTION

Attempts were first made to solve Eq. (23) numerically with all u, v and w. Since the initial values of v and w are unknown and they are assumed to be zero at the nozzle exit, we must calculate the values of

v and w at the first station by satisfying the z - momentum equation and equation of continuity. No stable numerical solutions of v and w have been obtained in this way and numerical integration can not proceed downstream. We are still trying to improve our numerical method in order to find stable numerical solution including the cross flow term. However from our successful numerical solutions of two dimensional and axisymmetrical jet reported in Part A, we find out that the influence of cross flow terms is not too strong on the distirbution of axial velocity distribution. If our main interest is the axial velocity distribution the following equation

$$\bar{u}\frac{\partial \bar{u}}{\partial x} = \frac{\partial^2 \bar{u}}{\partial y^2} + \frac{\partial^2 \bar{u}}{\partial z^2} \tag{24}$$

together with the proper initial and boundary condition (22) would give reasonable good results. We use bar to denote without cross flow. Hence we solve equation (24) numerically for axial velocity distribution with the initial and boundary condition (22). In order to check the accuracy of the approximation (24), we calculate also equation (24) for the two limiting cases; (i) two dimensional case $L = \infty$ and (ii) axisymmetrical case. Since we have the exact numerical solution for these two limiting cases in Part A, we may easily find out the accuracy of this approximation (24) by comparing the numerical results of Eq. (24) of these two limiting cases and the exact solutions with cross flow. We find the

accuracy is reasonable good. Since we expect that the general three dimensional results should lie between these two limiting cases, we may find a method of correction to improve the numerical results of three dimensional jet of Eq. (24) which will be discussed later.

X. RESULTS AND DISCUSSION

(a) Numerical computation. In Part A, $\Delta y = 0.05$ and $y/D = 20$ were used in the computation and satisfactory results were obtained. In the computation of three dimensional jet, due to the storage capacity of UNIVAC 1108, total grid point over a station can only have 70×70 . When $\Delta x = \Delta y = 0.1$ are used, we have $z/D = y/D = 7$. This means that the boundary is set at $7D$ away in the y- and z-direction. A check of using such a boundary and spacing in two dimensional and axi-symmetrical jets indicates poor result for $x > 1$. The central (maximum) velocity falls too rapidly for $x > 1$. However, for $x < 1$, the agreement with previous solution is good. To improve this result, we increase Δy and Δz to 0.2 and then the boundaries are at $y/D = z/D = 14$. Thus, we get better boundary conditions but sacrifice the accuracy in finite difference method. A check for two dimensional and axi-symmetric results shows that the center velocity is slightly lower by 0.01 to 0.02 in magnitude and the velocity profile is lower by the same amount near the central portion but agrees well in the tail. Most important is that the whole flow field is in better agreement with the exact solution.

Therefore, in our three dimensional jet calculation, both values $\Delta y = \Delta z = 0.1$ (for $x \leq 1$ only) and $\Delta y = \Delta z = 0.2$ were used. When we compare the numerical results for these two spacing values, it was found that the difference in center velocity is insignificant and the velocity profile shows a wider tail in z - direction when $\Delta y = \Delta z = 0.2$, were used with $x \geq 0.3$ and $L > 1$ but insignificant difference in the y - direction. Thus we feel that the spacing $\Delta y = \Delta z = 0.2$ used in the numerical integration is sufficient. The same program was applied to the three dimensional linearized equation and the numerical results agree satisfactorily with the analytic solution of reference 3.

(b) Central velocity (maximum velocity at each x - station). In Figure 14, numerical solution of the central velocity (without cross velocity) as a function of x - distance from nozzle exit are plotted for two dimensional, axisymmetrical and three dimensional jet with aspect ratio $L = 1$, 2 and 4 without free stream. It is interesting to note that the character of these curves are similar to those obtained from linearized equation[1]. For $L = 1$ (also axisymmetrical jet) and $L = 2$, no significent difference between the numerical solution and linearized solution was found. For large L , numerical solution gives higher center velocity. In Figure 14, exact numerical solutions with cross velocity for two dimensional and axisymmetrical jet are also shown.

We may figure out the correction factor due to neglecting the cross flow for two dimensional and axisymmetric jets by comparing the corresponding approximate and exact numerical solutions. Furthermore, since the two dimensional and axisymmetrical jets are two limiting cases of the three dimensional

jet, we may consider the correction factors of two dimensional and axisymmetrical jet as lower and upper bounds respectively for the correction factor of the three dimensional jet. The following correction factor for three dimensional jet is suggested.

Let u_{mo} and $u_{m\infty}$ be the center velocity with cross flow for axisymmetrical (subject o) and two dimensional (subscript ∞) jet respectively. Then $\bar{u}_{mo}$, $\bar{u}_{m\infty}$ and $\bar{u}_{mL}$ as well as c_{uo}, $c_{u\infty}$, c_{uL} be the central velocity without cross flow and correction factors for axisymmetrical, two dimensional and three dimensional (subscript L) jet with aspect ratio L respectively. We define

$$c_{uo} = \frac{u_{mo} - \bar{u}_{mo}}{u_{mo}} \quad , \quad c_{u\infty} = \frac{u_{m\infty} - \bar{u}_{m\infty}}{u_{m\infty}} \tag{25}$$

and

$$\Delta c_{uo} = c_{uo} - c_{u\infty} \quad , \quad c_{uo} > c_{u\infty} \tag{26}$$

$$\Delta u_{mo} = \bar{u}_{m\infty} - \bar{u}_{mo} \quad , \quad \Delta u_{mL} = \bar{u}_{m\infty} - \bar{u}_{mL} \quad . \tag{27}$$

Then

$$c_{uL} = \frac{\Delta u_{mL}}{\Delta u_{mo}} \cdot \Delta c_{uo} + c_{u\infty} \tag{28}$$

$$u_{mL} = \bar{u}_{mL}(1 + c_{uL}) \tag{29}$$

Figure 15 shows the correction factor c_{uL} as a function of distance from nozzle exit. The corrected central velocity for L = 1, 2 and 4 are shown in Figure 14.

(c) Axial velocity profiles. The axial velocity profiles for three dimensional jet without cross flow are shown in Figure 16 for $L = 1,\ 2$ and 4. In Figure 17, the errors introduced by neglecting the cross flow for two dimensional and axisymmetrical jets are shown by plotting $(u/\bar{u}) \ / \ (u_m/\bar{u}_m)$ where u and $\bar{u}$ denote axial velocity with and without cross flow respectively and subscript m denotes the value on the axis of the jet, i.e., u_m is the central velocity. It should be noted that even though the error at the tail is large but the effect is small because the magnitude of velocity at the tail is always very small.

Similarly, we may find the correction factor for the general velocity profile from the two dimensional and axisymmetrical jet results in the same manner as that for center velocity. The difference in error due to cross flow for two dimensional and axisymmetrical jets

$$\Delta = \left[\left(\frac{u_o}{\bar{u}_o}\right) \Big/ \left(\frac{u_{mo}}{\bar{u}_{mo}}\right)\right] - \left[\left(\frac{u_\infty}{\bar{u}_\infty}\right) \Big/ \left(\frac{u_{m\infty}}{\bar{u}_{m\infty}}\right)\right] \qquad (30)$$

is always small in the central portion but it may become large toward the tail where the magnitude of velocity is always small. Hence a correction curve based either on two dimensional or axisymmetrical jet should be sufficiently accurate for the three dimensional jet.

The shape of three dimensional jet varies with x and their contours of constant velocity over a station are different for different velocity. For the purpose of correction, the local shape of the three dimensional jet plays

an important role. For simplicity, the contour of half-width ($u=u_m/2$) is chosen as the representative shape of jet for all velocities over a given x-station. The contours of half-width for three dimensional jet without cross flow are shown in Figure 18. The following rules are suggested for the correction of three dimensional jet due to cross flow effects:

(i) For plane perpendicular to y-z plane with largest half-width $\bar{b}_{1m}$, behaves like an axisymmetrical jet.

(ii) For other planes perpendicular to y-z plane half-width $\bar{b}_1$ approaches to two dimensional jet linearly proportional to $\bar{b}_1/\bar{b}_{1m}$, we have

$$\frac{(u_L/\bar{u}_L)}{(u_{mL}/\bar{u}_{mL})} = \frac{(u_\infty/\bar{u}_\infty)}{(u_{m\infty}/\bar{u}_{m\infty})} + \frac{\bar{b}_1}{\bar{b}_{1m}}\Delta \qquad (31)$$

where Δ is given by Eq. (30). Since $(u_{mL}/\bar{u}_{mL})$ is given in Eq. (29) and $\bar{u}_L$ as well as all terms on the right-hand side of Eq. (31) are known, we may calculate the value u_L. We feel that this correction is sufficient accurate even though the correction scheme is somewhat arbitrary.

(d) Half-width of the three dimensional jet. The contours of half-width of three dimensional jet with $L = 1$, 2 and 4 without cross flow are shown in Figure 18. The correction factors due to cross flow are shown in Figure 15 which were obtained in a similar manner as other correction factors from the exact solutions of two dimensional and axisymmetrical jet. The difference of these correction factors for the two limiting cases is small.

XI. CONCLUSIONS AND GENERAL REMARKS

From our numerical solutions, the following conclusions may be drawn:

(1) Numerical solutions for two dimensional and axisymmetrical free jets give better description of the flow field than similarity solutions as compared with the existing experimental data. The boundary layer equation is a good approximation for the free jet problem provided that the Reynolds number at nozzle exit is not too low.

(2) For two dimensional and axisymmetrical jets, parabolic initial velocity distribution gives better agreement between numerical and similarity solutions. The approach of numerical solution at large x to similarity solution is demonstrated clearly in both central velocity and velocity profile.

(3) When the jet velocity deviates slightly from the uniform free stream velocity, the numerical solutions agree with the results of linearized theory. For instance, when the jet velocity is 1/10 greater than the free stream value, the difference between numerical and linearized solutions is of the order of 0.001 to 0.002 of the free stream velocity. With free stream, the magnitude of the cross flow is reduced significantly.

(4) The axial velocity distributions of the three dimensional jet issuing from a rectangular nozzle of various aspect ratio without free stream have been calculated numerically by neglecting the cross velocity ($v = w = 0$). The correction factors due to cross flow have been obtained from the exact solutions with cross flow of two dimensional and axisymmetrical jet.

(5) The central velocity given by non-linear equations is higher than the corresponding linearized equation and the spread of non-linear jet is much greater than the linearized case.

(6) The effects of neglecting the cross flow are to lower the center velocity and to increase the velocity in the tail.

(7) Although no experimental data available for the three dimensional jet, from the results of the two dimensional and the axisymmetrical jet, we feel that our three dimensional jet numerical solutions are sufficiently accurate.

(8) Further development of numerical scheme to include the cross flow for three dimensional jet is still needed, because in our approximate numerical solution, no information about cross velocity components for three dimensional jet is given.

REFERENCES

1. Pai, S. I., *Fluid Dynamics of Jets*, D. Van Nostrand Co., Inc., Princeton, New Jersey, 1954.

2. Abramovich, G. N., *The theory of turbulent jet*, M. I. T. Press, 1963.

3. Pai, S. I. and Hsieh, T. Y., *Three Dimensional Laminar Jet Mixing*, Physics of Fluids, Vol. 12, No. 4, April, 1969, pp. 936-937.

4. Flugge-Lotz, I. and Blottner, F. G., *Numerical Solution of Compressible Boundary Layer*, Div. of Eng. Mech., Stanford University, TR 131, January, 1962.

5. Chanand, R. C. and Powell, A., *Experiments Concerning the Sound-Sensitive Jet*, Jour. of Accou. Soc. of America, Vol. 34, No. 7, p. 907, July, 1962.

6. Sato, H. and Sakao, F., *An Experimental Investigation of the Instability of A Two-dimensional Jet at Low Reynolds Numbers*, Jour. of Fluid Mech., Vol. 20, No. 2, p. 337, 1964.

7. Andrade, E. N. Da C. and Tsien, L. C., *The Velocity Distribution in a Liquid-Into-Liquid Jet*, Proc. Phy. Soc., London, Vol. 49, P. 381, 1937.

8. Peaceman, D. W. and Rachford, H. H., Jr., *The Numerical Solution of Parabolic and Elliptic Differential Equations*, Jour. Soc. Ind. Appl. Math., Vol. 3, pp. 28-41, 1955.

APPENDIX I

In the implicit finite difference method described in Part A for two dimensional and round jet and Part B for three dimensional jet, u-component in the new station must be obtained by solving a set of N-1 simultaneous algebraic equations as follow:

$$B_1 u_1 + c_1 u_2 = D_1 \qquad r = 1$$

$$A_r u_{r-1} + B_r u_r + c_r u_{r+1} = D_r \qquad 1 < r < N-2$$

$$A_{N-1} u_{N-2} + B_{N-1} u_{N-1} = D_{N-1} \qquad r = N-1$$

where N is the total number of grid points in one direction, A, B, C and D are coefficients. Treat A, B, C and D as vectors of N-1 component and let α, β and γ be the new vectors of N-1 component and

$$\alpha_1 = \beta_1$$

$$\alpha_r = B_r - A_r \beta_{r-1} \qquad 2 < r \leq N-1$$

$$\beta_r = \alpha_r^{-1} c_r \qquad 1 \leq r \leq N-1$$

$$\gamma_1 = \alpha_1^{-1} D_1$$

$$\gamma_r = \alpha_r^{-1} (D_r - \gamma_{r-1} A_r) \qquad 2 \leq r \leq N-1$$

It can be shown that

$$u_{N-1} = \gamma_{N-1}$$

$$u_r = \gamma_r - \beta_r u_{r+1} \qquad 1 \leq r \leq N-2$$

Thus α, β, γ are calculated in order of increasing r and u is obtained in order of decreasing r. For proof, see Reference 4.

A computer program for two dimensional jet with rectangular initial velocity distribution is given below:

```
C       Two Dimensional Jet, Numerical Calculation (Implicit Method)
        Dimension U(800), UP(800), B(800), V(800), AM(800), AN(800),
        AU(800), ID(800), AHI(10), LI(10), A(800), C(800)

C       STEP  INITIAL VEL. DISTRIBUTION AT THE EXIT

9900    READ(5,1100) NY, NYE, LL, KY, KY1, KY2, KY3, LY, P, UO, XST
        WRITE (6,1100) NY, NYE, LL, KY, KY1, KY2, KY3, LY, P, UO, XST

1100    FORMAT (815, 3F10.5)
        READ (5,3100) (LI(N), N=1, LL)
        WRITE(6,3100) (LI(N), N=1, LL)

3100    FORMAT(1015)
        READ(5,3200) (AHI(N), N=1, LL)
        WRITE(6,3200) (AHI(N), N=1, LL)

3200    FORMAT(3F10.6, 7F6.5)
        NY1 = NY + 1
        NYE = NY - 1
        KD = KY - 1
        DO 51 I = 1, NY1
        IF(I-NYE) 501, 501, 503

501     UP(I) = 1
        GO TO 51

503     UP(I) = 0.

51      CONTINUE
        WRITE(6, 1009)

1009    FORMAT(30H INITIAL VELOCITY DISTRIBUTION,/)
        WRITE(6,1006)
        WRITE(6,1000) (UP(I), I = 1, NY1, LY)
        WRITE(6,1001)
        X = 0
        UP(NYE) = .5
        P2 =  P**2
        KYP = 10
        DO 9800 KL = 1, LL
        L = LI(KL)
        AH = AHI(KL)
        DO 9000 KKK = 1,L
        X = X + AH
        IF(UO) 81, 82, 81
```

```
82          XPM = 0
            GO TO 83

81          XPM = X/UO

83          DO 9200 K = 1, KYP
            DO 9100 KA = 1, KY1
            DO 17 M = 1, NY1
            IF(KA - 1) 201, 201, 202

201         UCO=UP(M) + UO
            GO TO 203

202         UCO=U(M) + UO

203         B(M)=P2*UCO/AH+2.

17          D(M)=UCO*P2*UP(M)/AH                    #1
            AM(1)=B(1)
            AN(1)=-2./AM(1)
            AU(1)=D(1)/AM(1)
            DO 15 M=2,NY
            AA=-(.5*P*V(M) + 1)                     #2
            CA=(.5*P*V(M) - 1)                      #3
            AM(M)=B(M) - AA*AN(M-1)
            AN(M)=CA/AM(M)

15          AU(M)=(D(M) - AU(M-1)*AA)/AM(M)
            IF(KA - KY1) 305, 306, 306

306         DO 61 M = 1, NY1

61          B(M) = U(M)

305         U(NY) = AU(NY)
            DO 14 M = 1, NYR
            MM = NY - M

14          U(MM)=AU(MM)-AN(MM)*U(MM+1)

9100        CONTINUE
            DO 63 M = 1, NY

63          U(M) = .5*(B(M) + U(M))
            V(1) = 0.
            SUM = (U(1) - UP(1))/AH                 #4
            DO 29 M = 2, NY1
            DDT=(U(M) - UP(M))/AH                   #5
            SUM=SUM + 2.*DDT
29          V(M) = -(SUM - DDT)*.5*P                #6
            KY1 = KY2
            IF(KYP - 1) 9200, 9200, 309
```

```
309       IF(K-KD) 9200, 308, 9200

308       DO 67 M=1, NY1
          C(M) = V(M)

67        A(M) = U(M)

9200      CONTINUE
          DO 68 M = 1, NY1
          V(M) = .5*(C(M) + V(M))

68        U(M) = .5*(U(M) + A(M))
          WRITE(6,1016) X, XPM

1016      FORMAT(/,30H AVERAGE VALUE FOR U, V AT X=,F9.5,5X,4H X'=,F9.5,/)
          WRITE(6,1006)
          WRITE(6,1000) (U(I),I=1,NY1,LY)
          WRITE(6,1007)
          WRITE(6,1000)(V(I),I=1,NY1,LY)

601       DO 65 M=1, NY1

65        UP(M) = U(M)
          IF(X-XST) 9000, 402, 402

402       KYP = KY

9000      CONTINUE
          IF(KL-1) 9800, 401, 401

401       KY1=KY3
          KY2=KY3

9800      CONTINUE
          WRITE(6,9500)

9500      FORMAT(1H1)
          GO TO 9900

1000      FORMAT(10F12.5)

1001      FORMAT(//)

1006      FORMAT(12H U COMPONENT, /)

1007      FORMAT(/,12H V COMPONENT,/)

          END
```

where NY = total number of grid point in y direction minus 1.

NYE = grid point at edge of exit

LL = number of sets of equal spacing stations to be calculated

KY = number of iteration for v at downstream X^* > XST

KY1, KY2, KY3 = number of iteration for u at first section, first set of stations and following stations respectively

LY = grid point in interval for printing

p = spacing in y direction

Uϕ = free stream velocity (U_o/U_j)

XST = distance from exit, for X^* < XST iteration in v is 10; for X^* < XST iteration in v is given by KY.

LI(LL) = number of stations to be calculated in each set

AHI(LL) = spacing between stations in each set

Transform from two dimensional case to axisymmetrical case can easily be done by changing the statements with # sign as follow:

#1 By adding a statement immediately next to it

```
B(1) = B(1) + 2
```

#2 `AA = -(.5*P*(V(M) - 1/((M-1)*P)) + 1)`

#3 `CA = .5*P*(V(M) - 1/((M-1)*P)) - 1`

#4 MULTIPLYING BY 0.5 ON THE R.H.S.

#5 MULTIPLYING BY (M-1) ON THE R.H.S.

#6 DIVIDING BY (M-1) ON THE R.H.S.

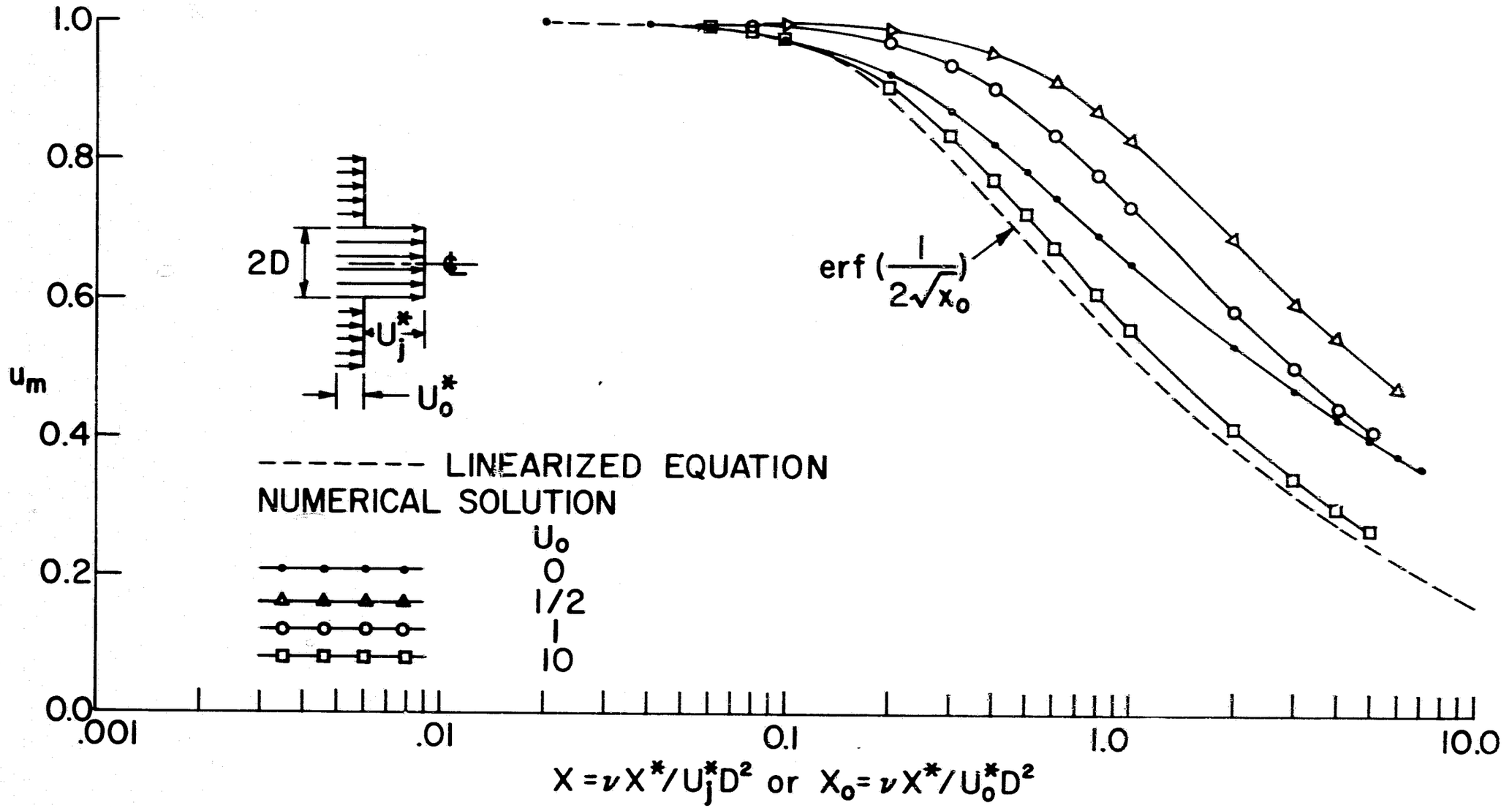

FIG. I. CENTRAL VELOCITY AS A FUNCTION OF DISTANCE FROM EXIT, TWO DIMENSIONAL JET.

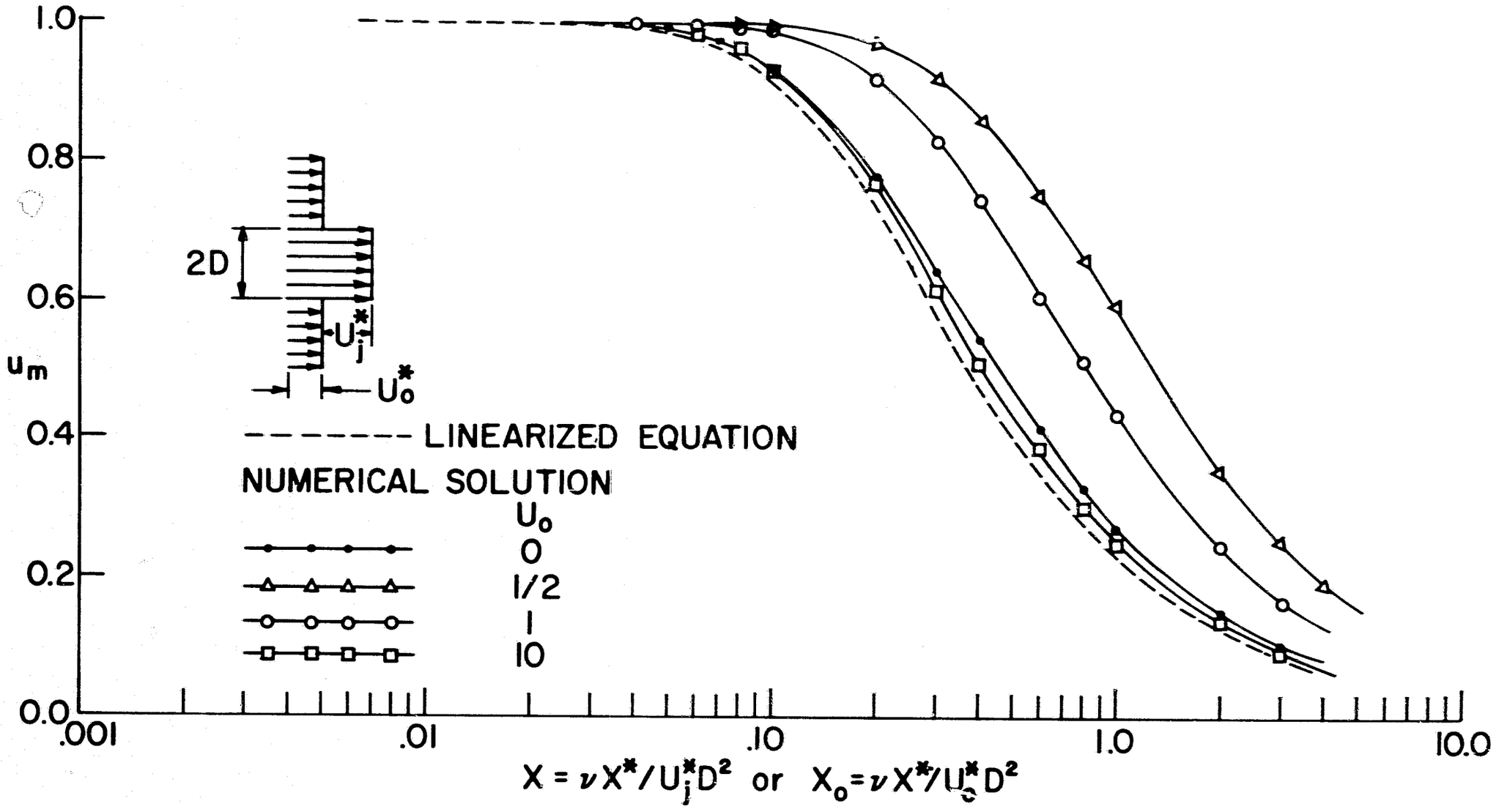

FIG. 2. CENTRAL VELOCITY AS A FUNCTION OF DISTANCE FROM EXIT, AXISYMMETRICAL JET.

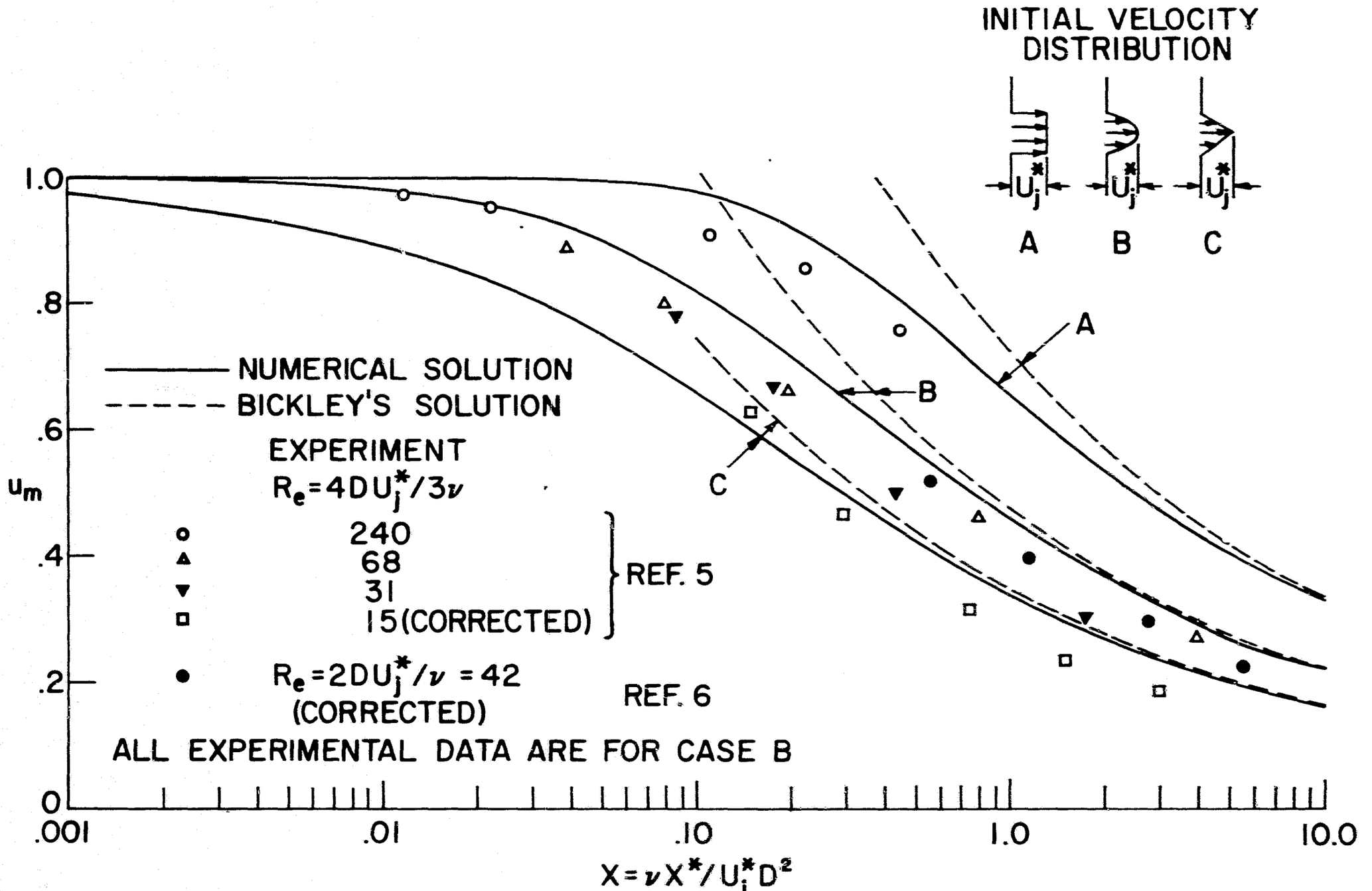

FIG. 3. CENTRAL VELOCITY AS A FUNCTION OF DISTANCE FOR VARIOUS INITIAL VELOCITY DISTRIBUTIONS AT EXIT, TWO DIMENSIONAL JET WITH AMBIENT FLUID STILL.

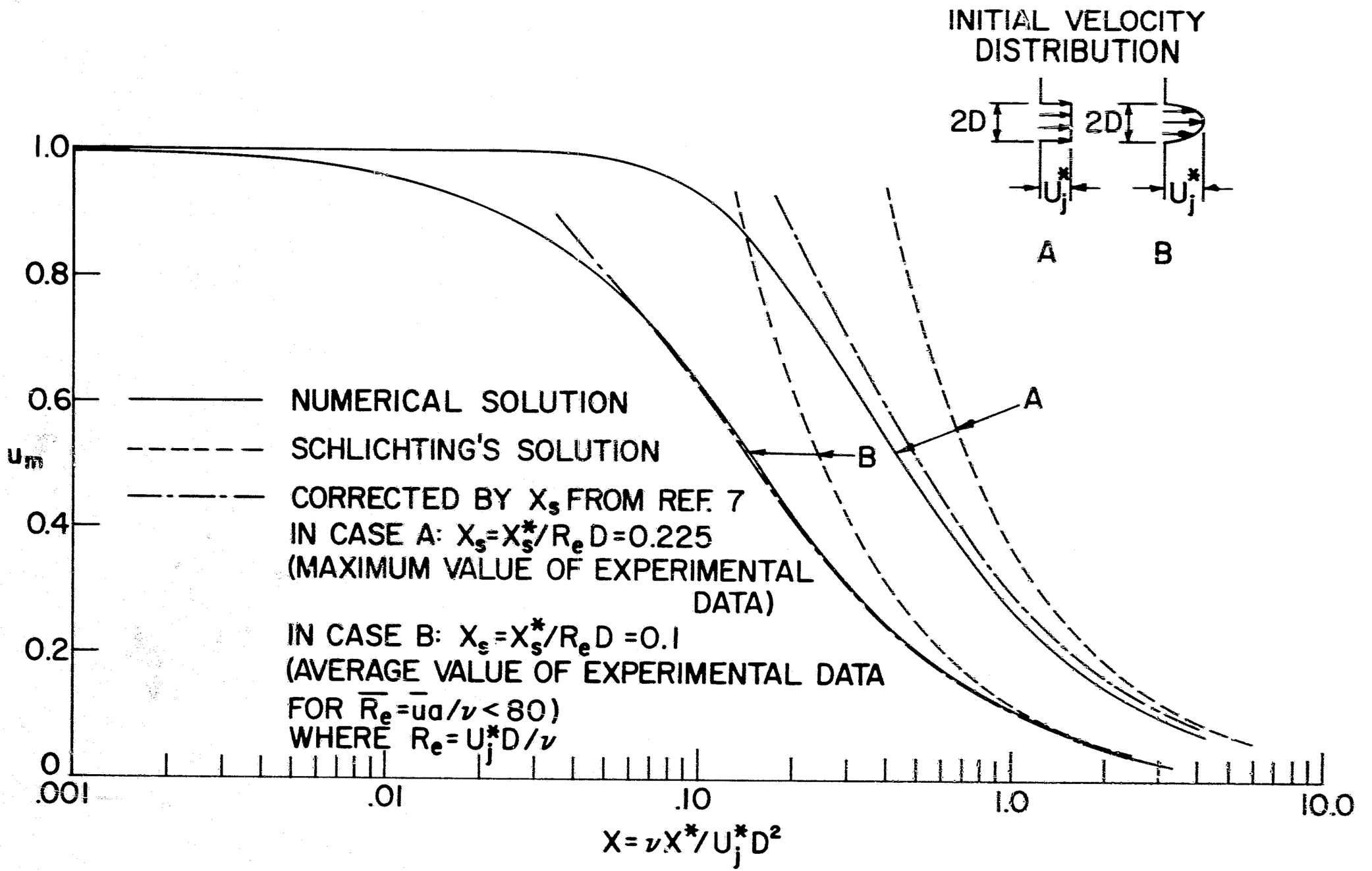

FIG. 4. CENTRAL VELOCITY AS A FUNCTION OF DISTANCE FOR VARIOUS INITIAL VELOCITY DISTRIBUTIONS AT EXIT, AXISYMMETRICAL JET WITH AMBIENT FLUID STILL.

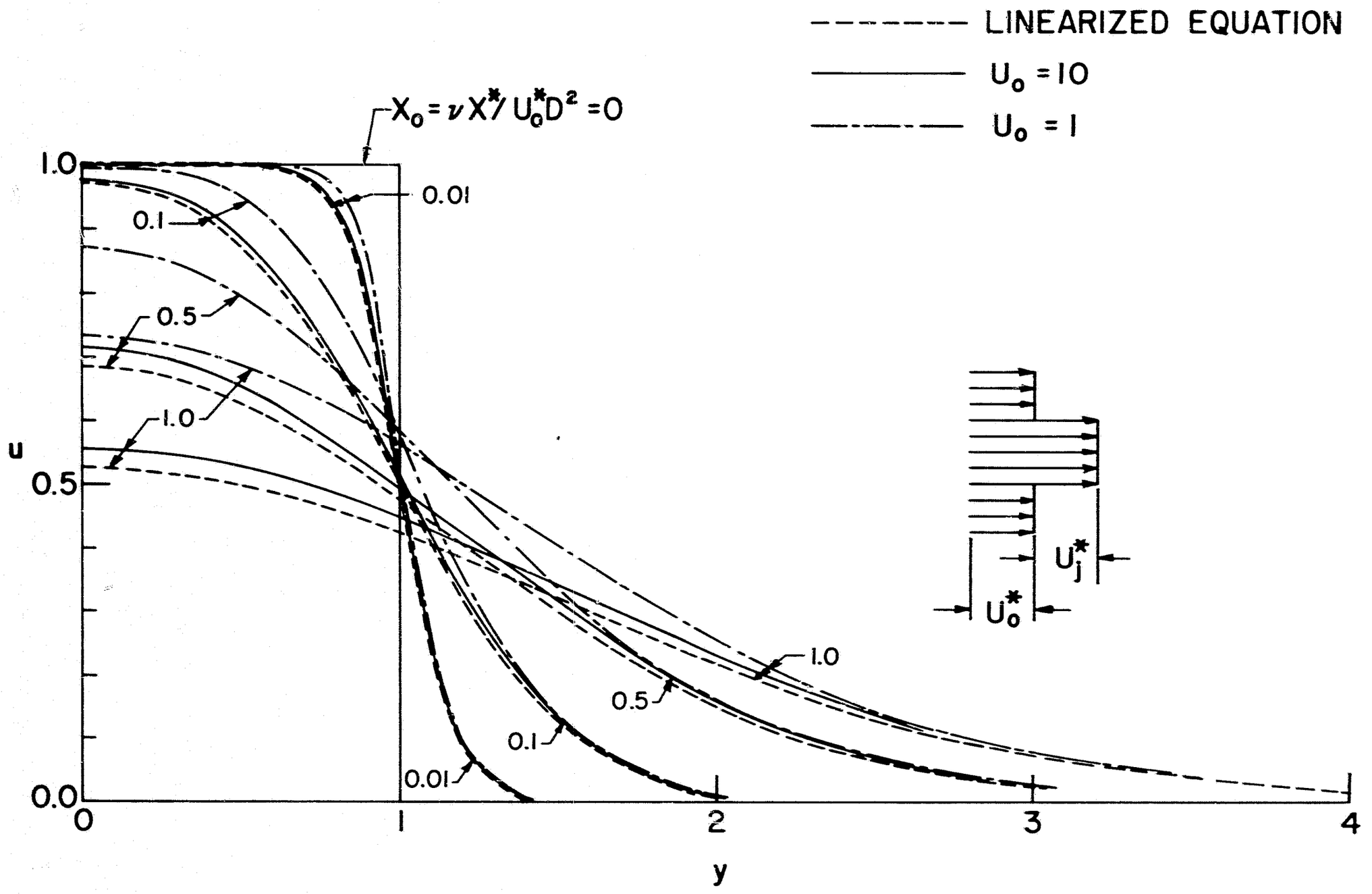

FIG. 5. VELOCITY PROFILES FOR TWO DIMENSIONAL JET WITH MOVING STREAM.

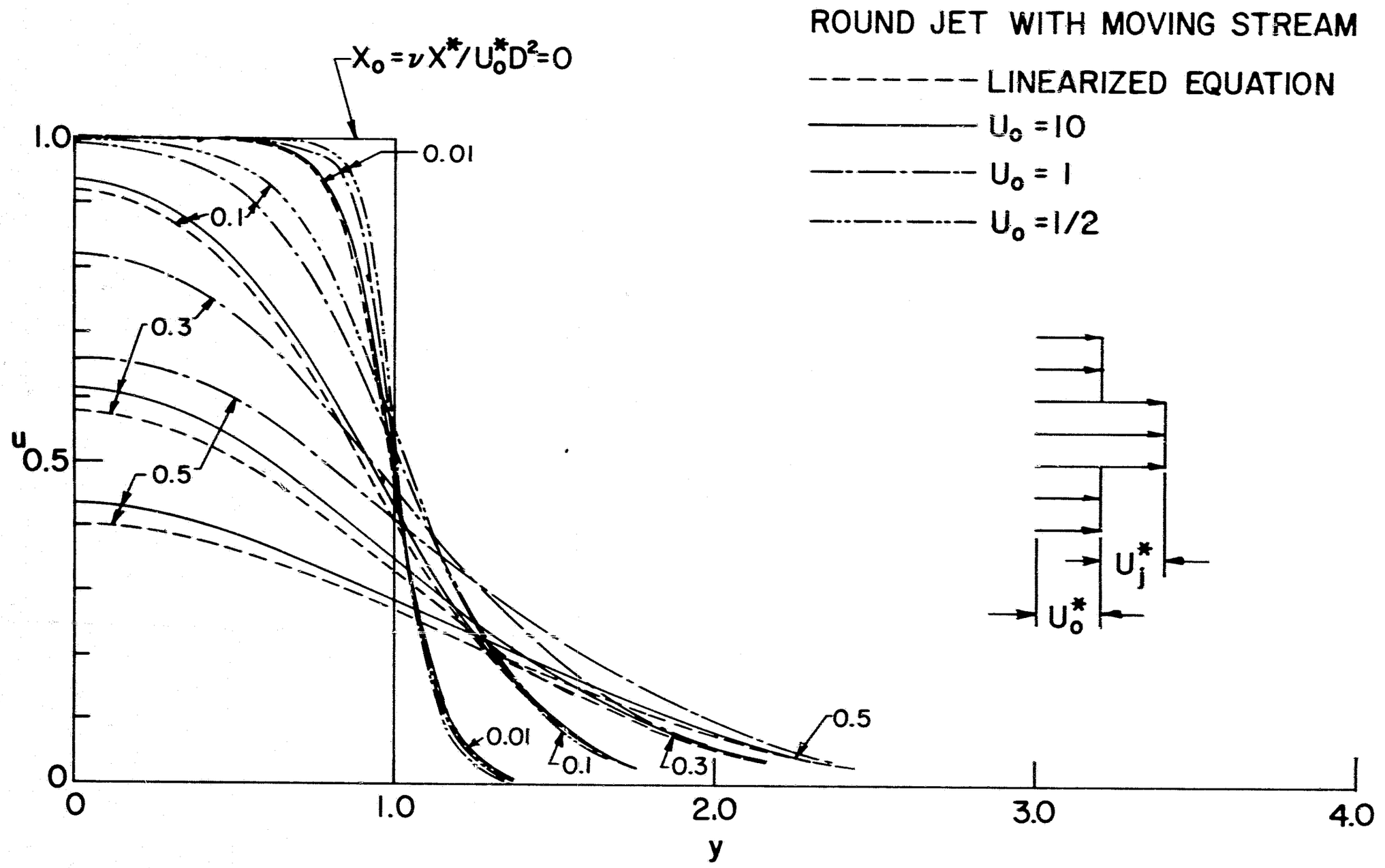

FIG. 6. VELOCITY PROFILES FOR AXISYMMETRICAL JET WITH MOVING STREAM.

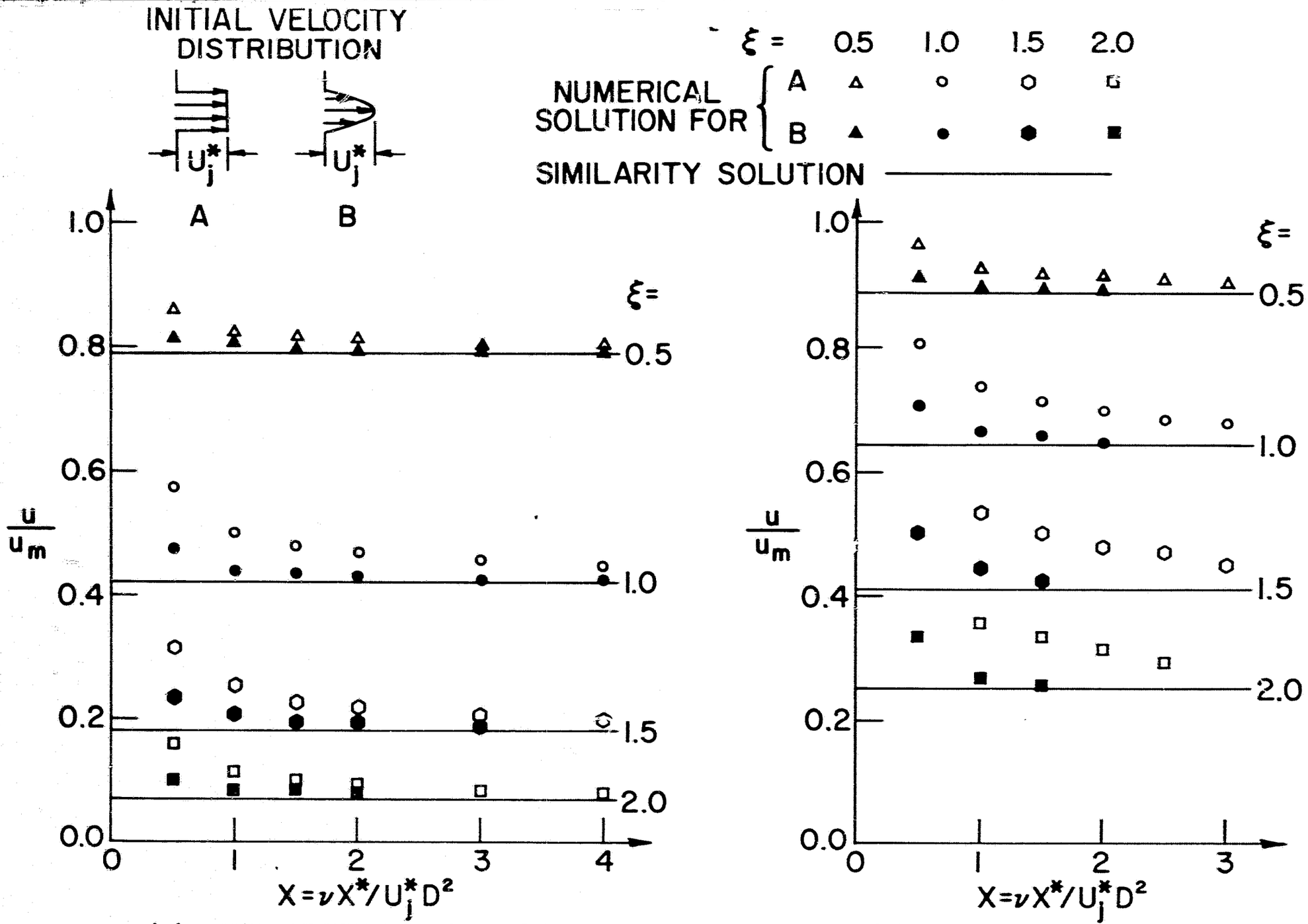

FIG. 7. COMPARISON OF u/u_m BETWEEN NUMERICAL AND SIMILAR SOLUTION AS A FUNCTION OF DISTANCE FROM EXIT.

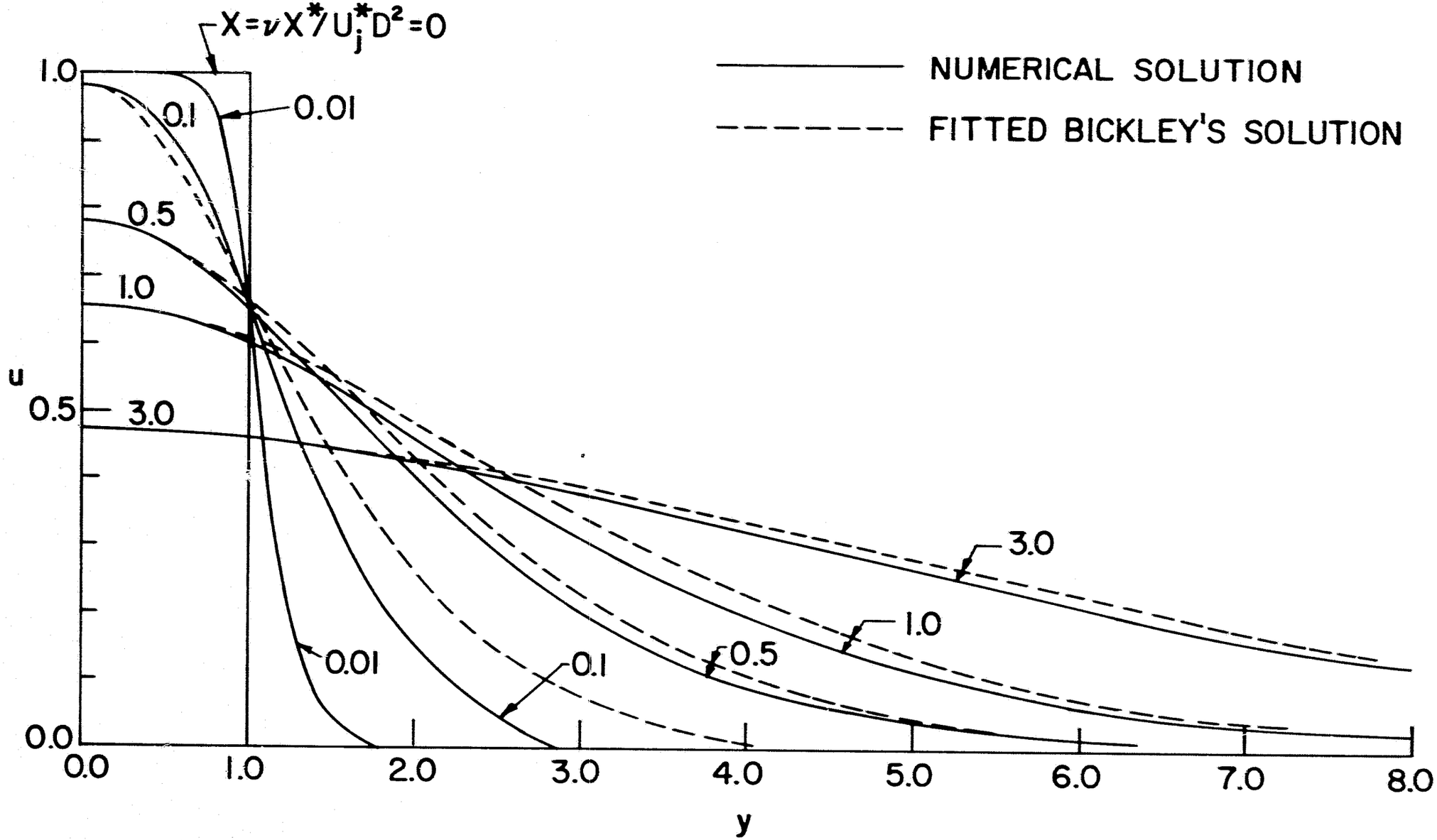

(A). RECTANGULAR INITIAL VELOCITY DISTRIBUTION.

FIG. 8. COMPARISON OF VELOCITY PROFILES BETWEEN NUMERICAL AND SIMILAR SOLUTION AT CONSTANT MOMENTUM FOR TWO DIMENSIONAL JET WITH AMBIENT FLUID STILL.

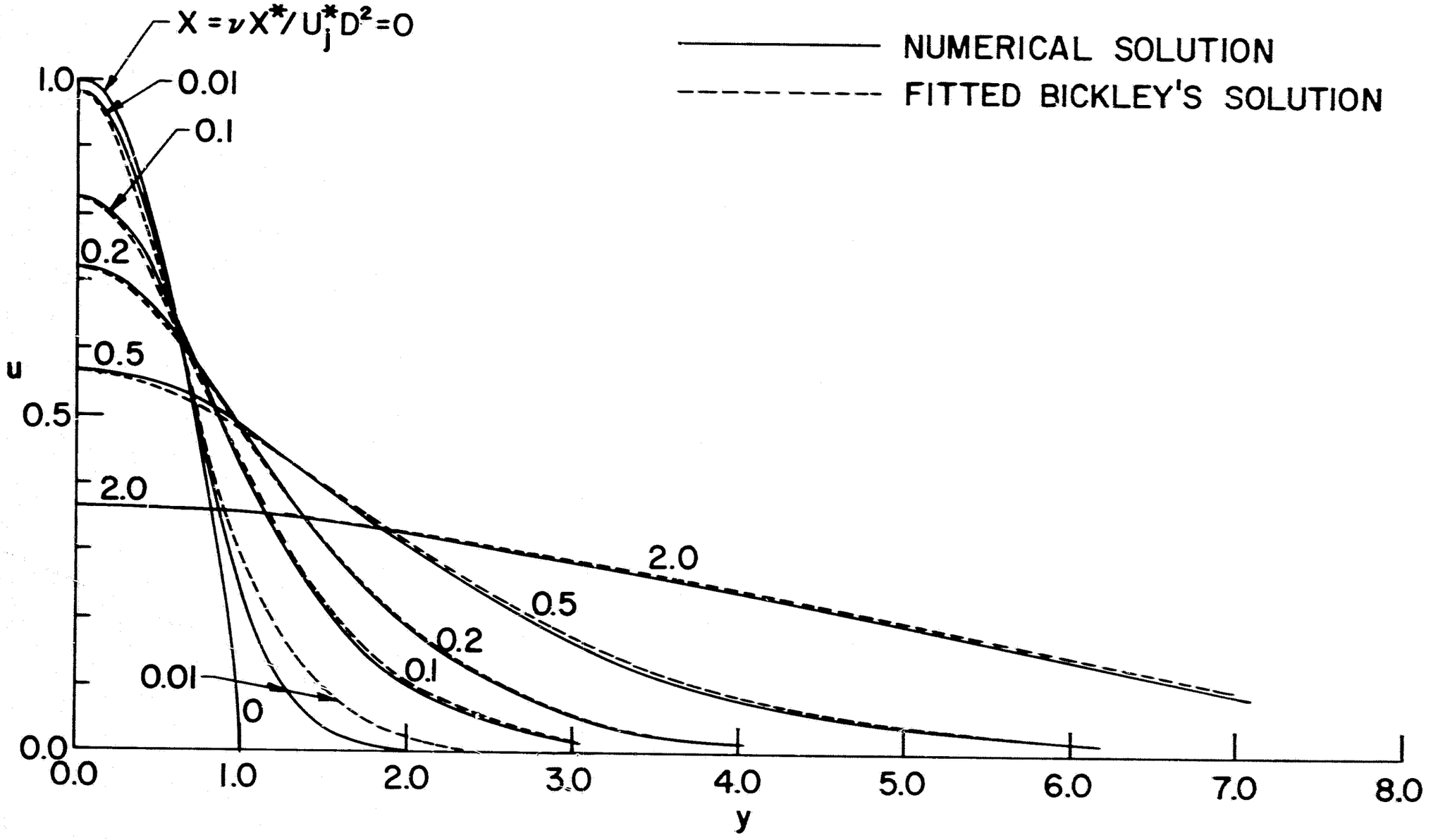

(B). PARABOLIC INITIAL VELOCITY DISTRIBUTION.

FIG. 8. CONCLUDED.

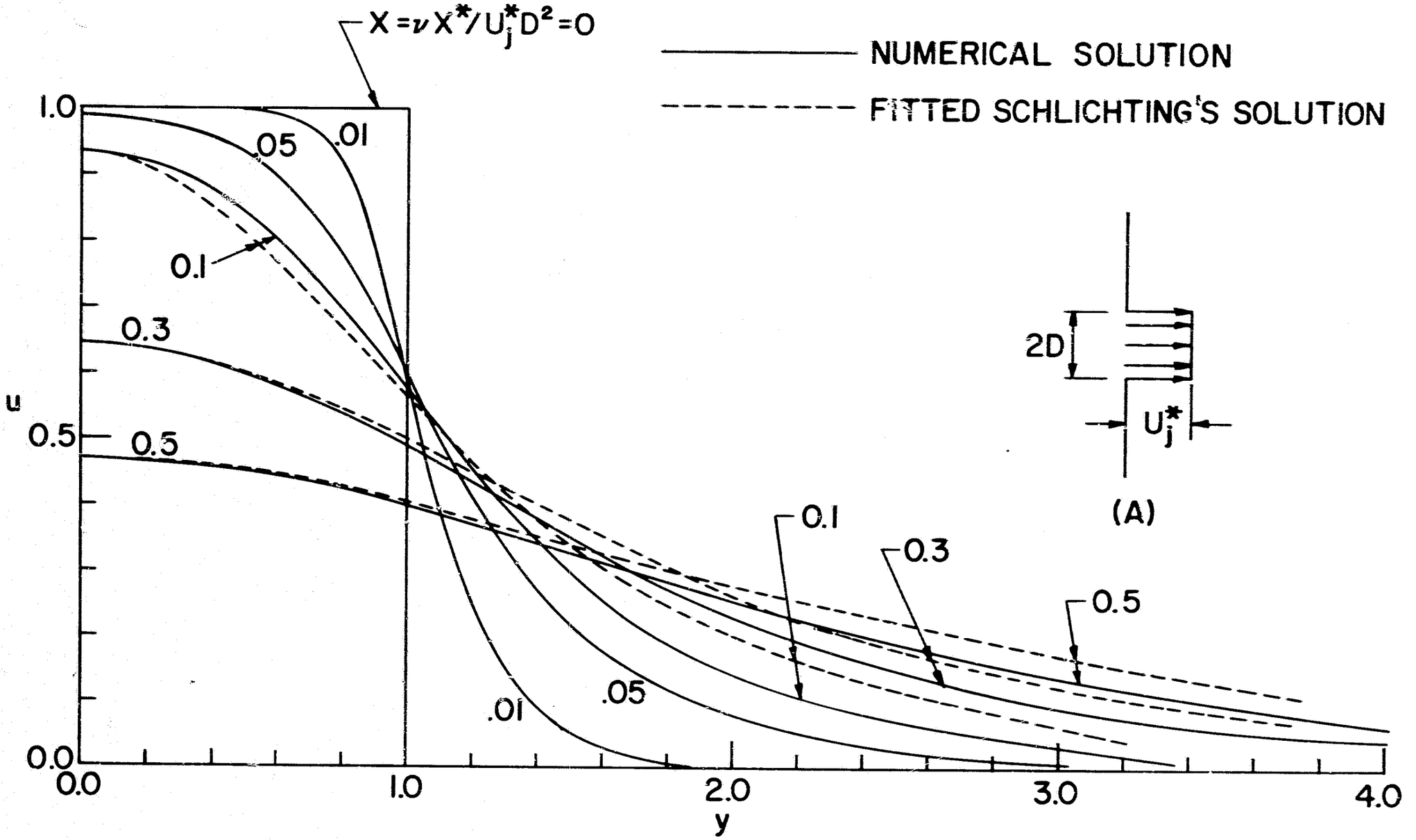

(A). RECTANGULAR INITIAL VELOCITY DISTRIBUTION.

FIG. 9. COMPARISON OF VELOCITY PROFILES BETWEEN NUMERICAL AND SIMILAR SOLUTION AT CONSTANT MOMENTUM FOR AXISYMMETRICAL JET WITH AMBIENT FLUID STILL.

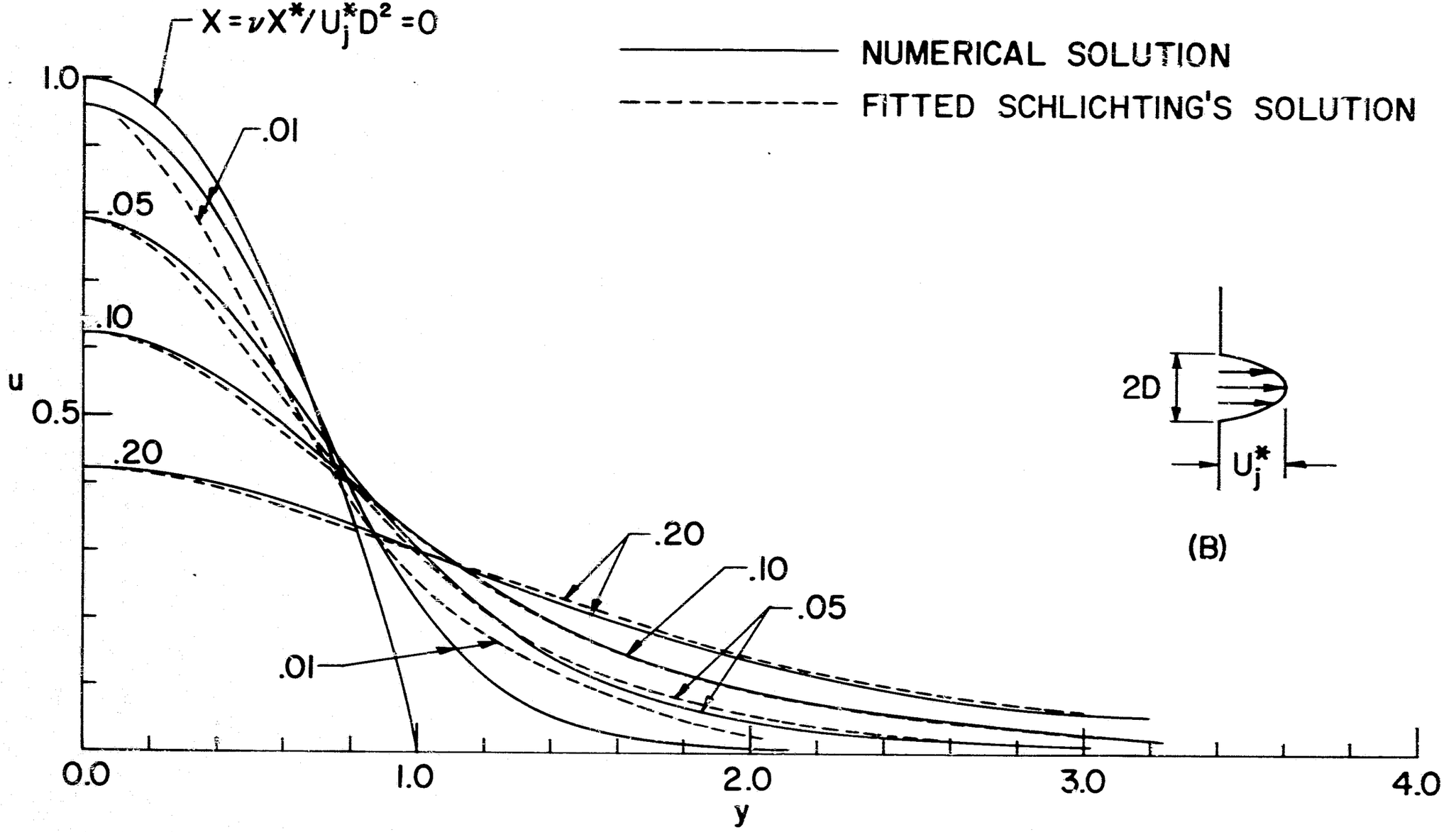

(B). PARABOLIC INITIAL VELOCITY DISTRIBUTION.

FIG. 9. CONCLUDED.

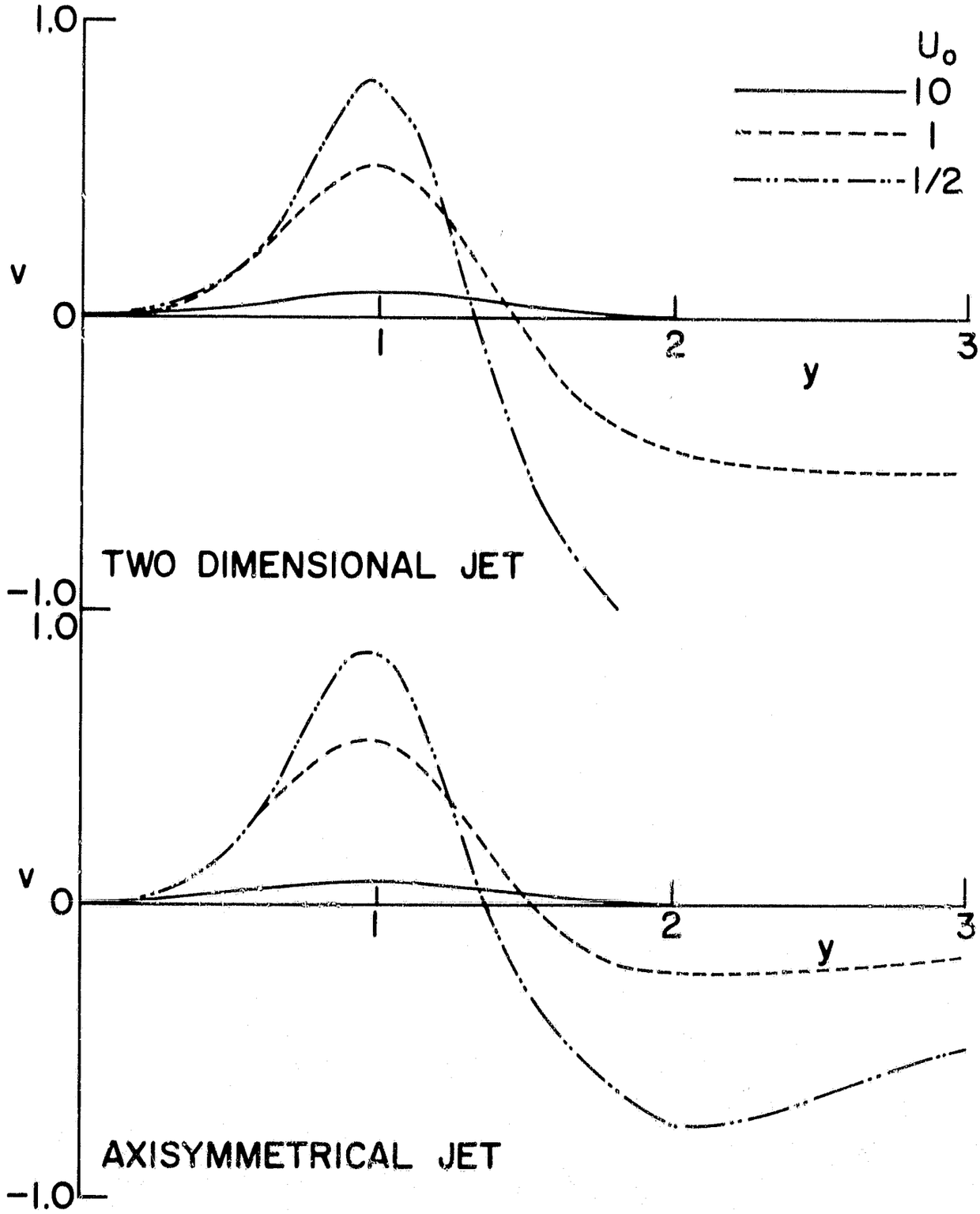

FIG. 10. VERTICAL VELOCITY DISTRIBUTION AT X_o=0.1 FOR JETS WITH MOVING STREAM, RECTANGULAR INITIAL VELOCITY DISTRIBUTION.

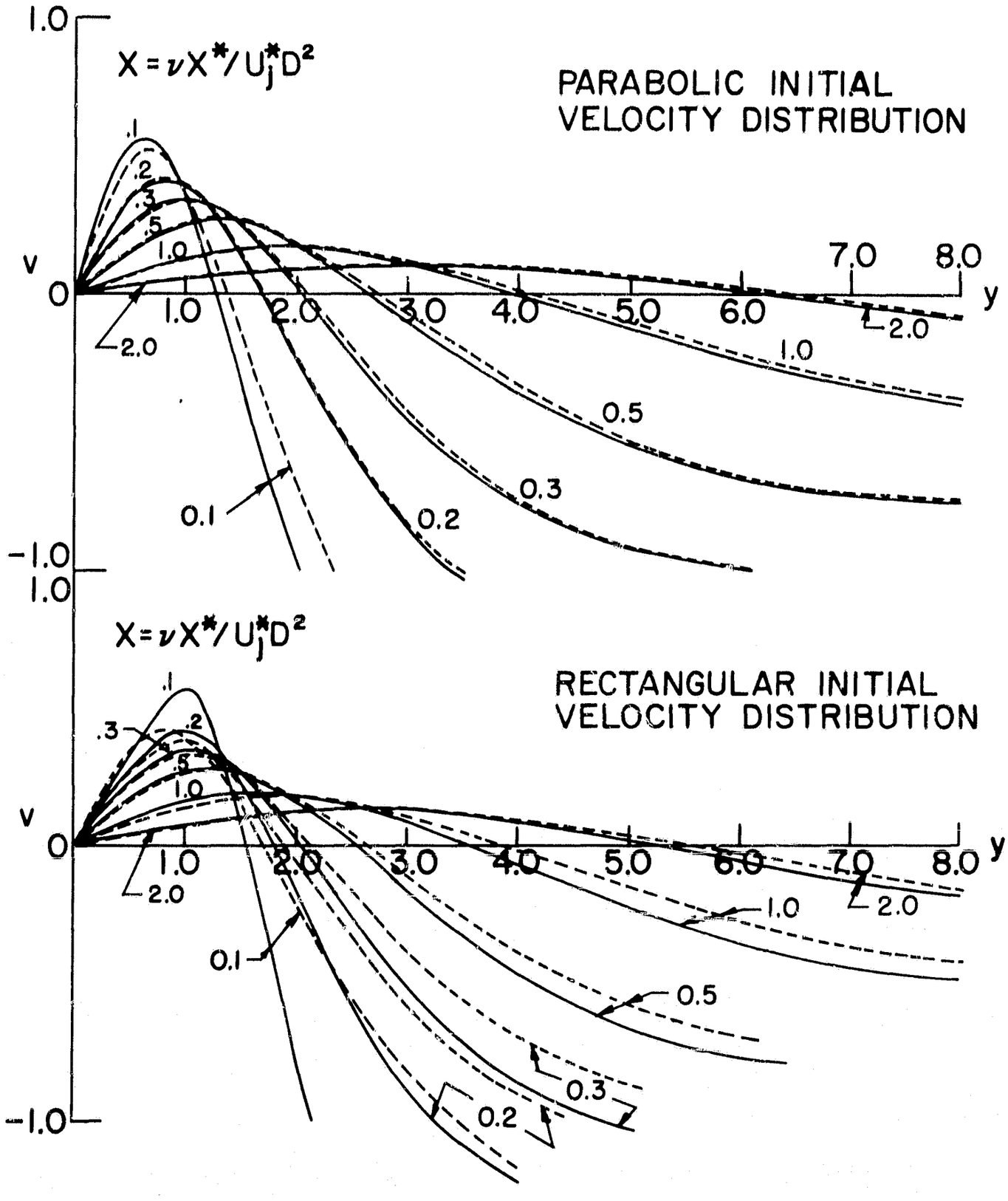

FIG. 11. VERTICAL VELOCITY DISTRIBUTION FOR TWO DIMENSIONAL JET WITH AMBIENT FLUID STILL.

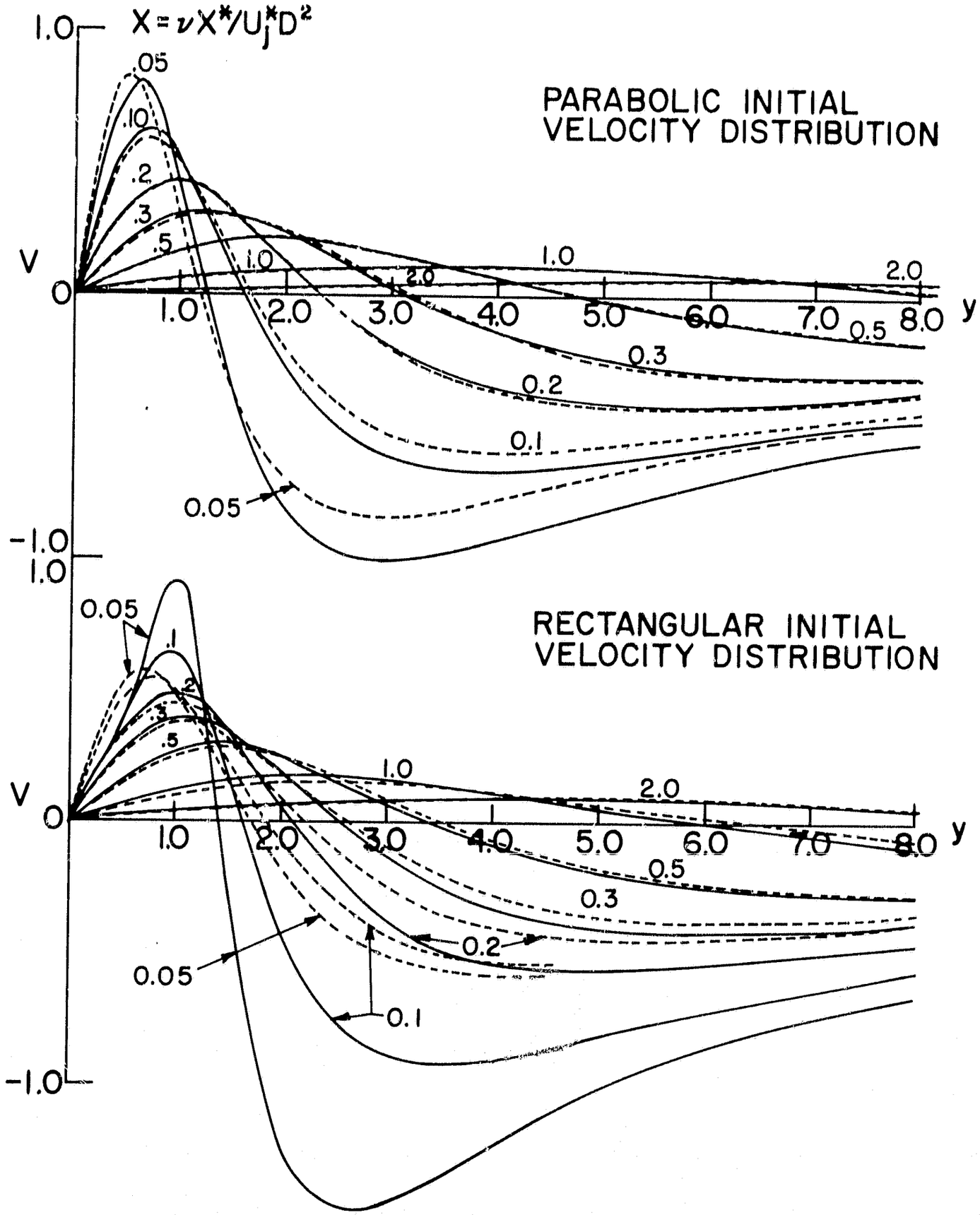

FIG. 12. VERTICAL VELOCITY DISTRIBUTION FOR AXISYMMETRICAL JET WITH AMBIENT FLUID STILL.

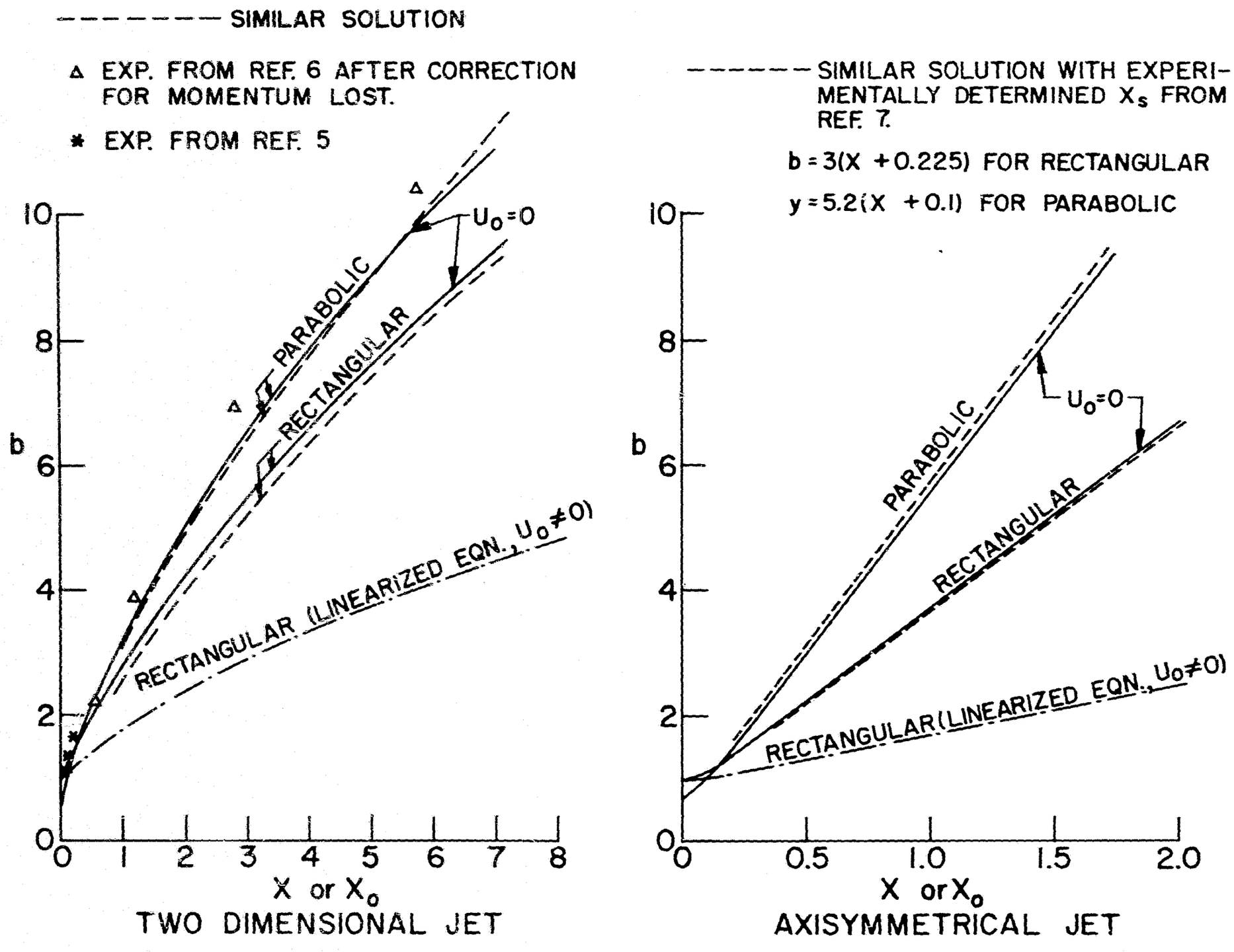

FIG. 13. THE SPREAD OF HALF WIDTH OF JETS.

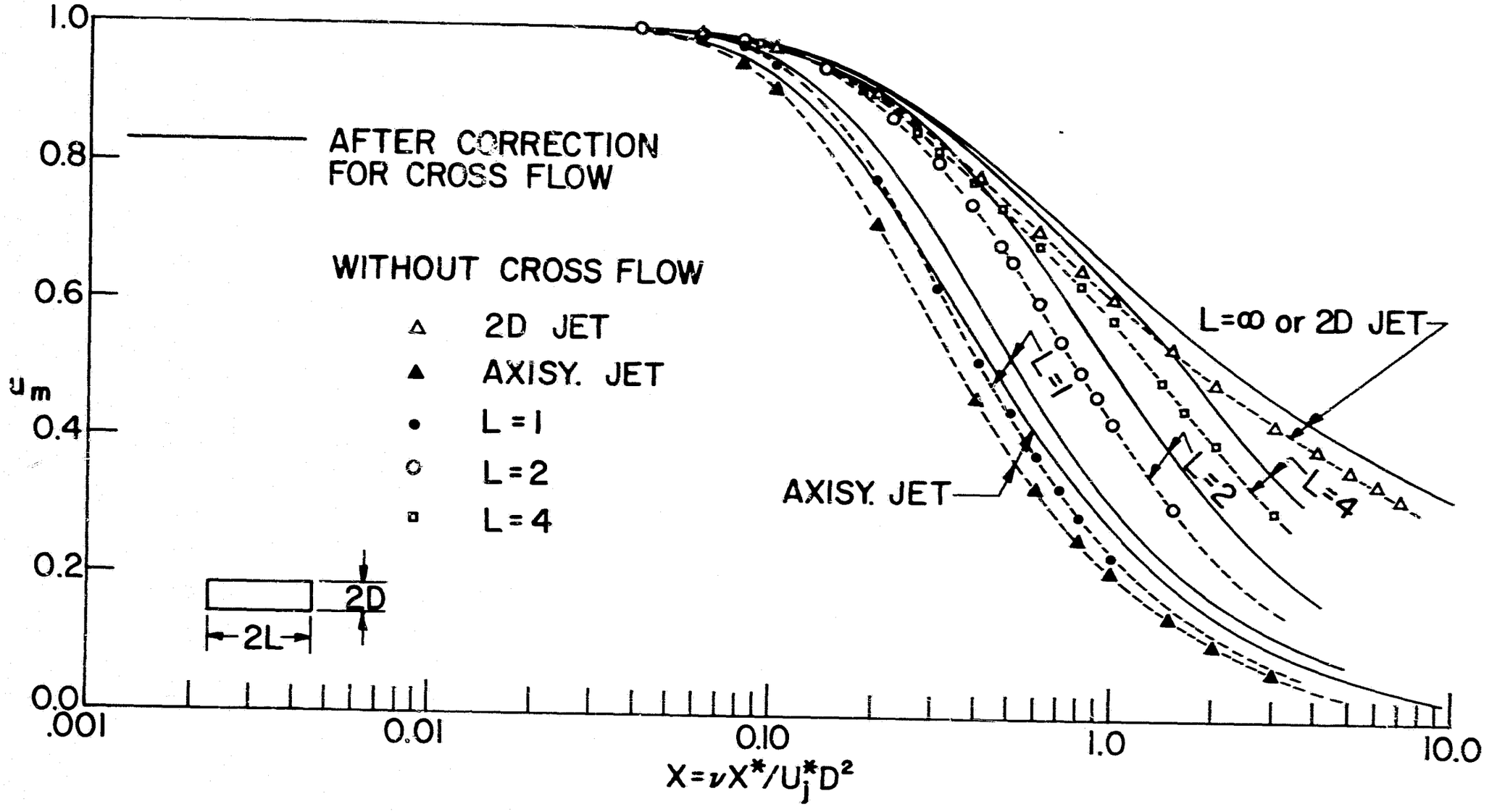

FIG. 14. CENTER VELOCITY OF THREE DIMENSIONAL RECTANGULAR JET AS A FUNCTION OF DISTANCE FROM EXIT.

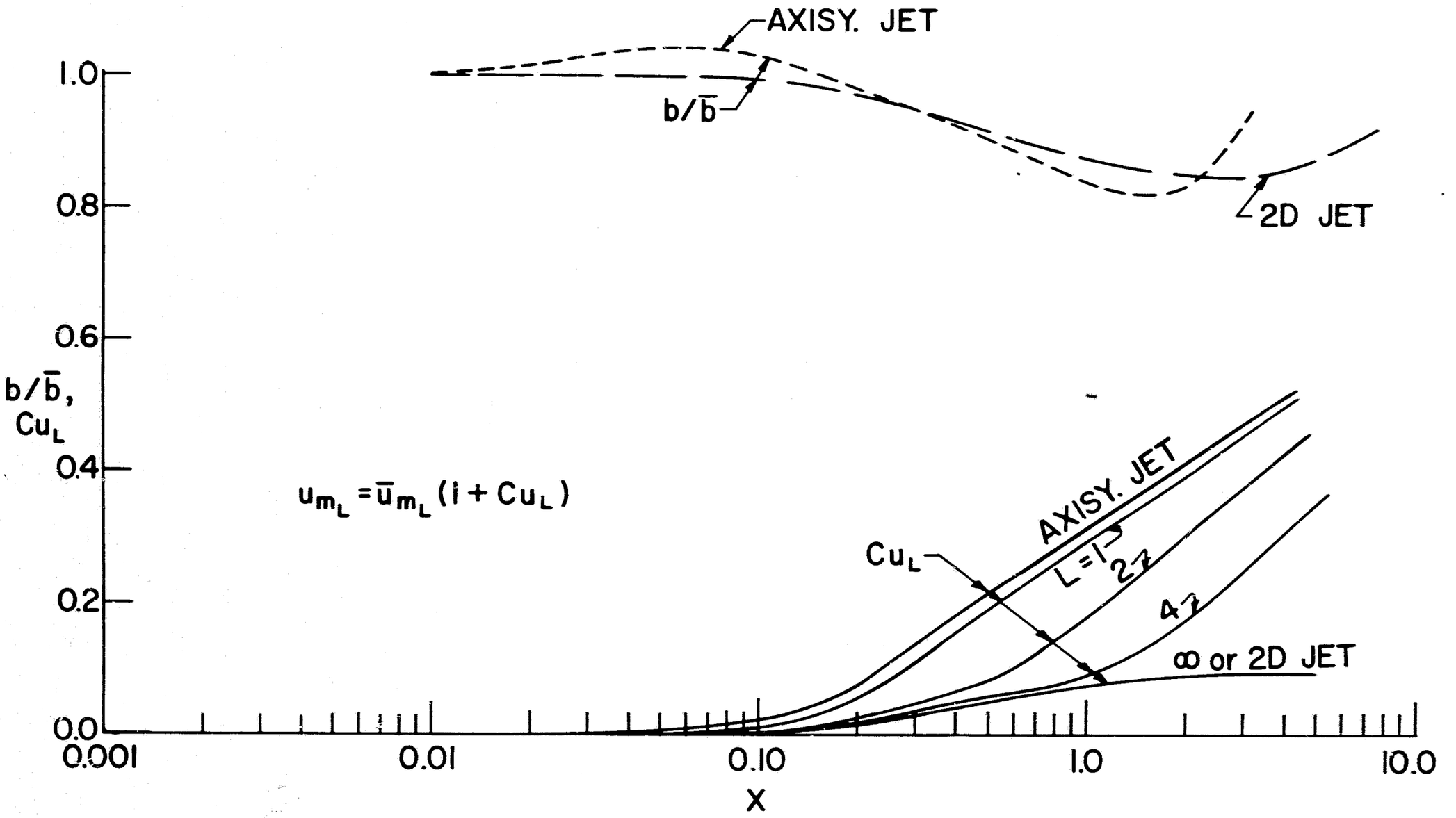

FIG. 15. THE CORRECTION FACTOR Cu_L AND HALFWIDTH RATIO $b/\bar{b}$ AS A FUNCTION OF DOWNSTREAM DISTANCE FROM EXIT.

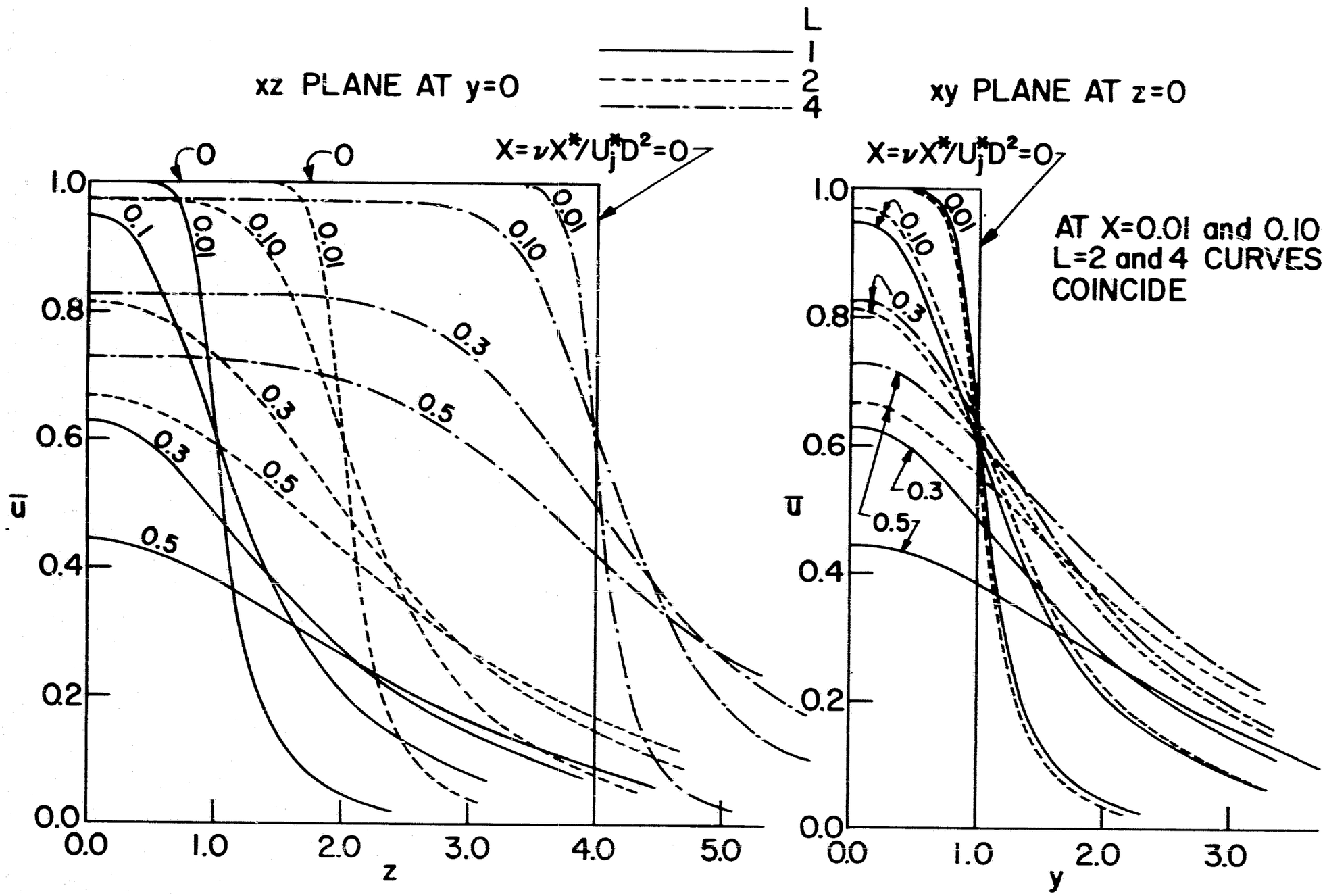

FIG. 16. VELOCITY PROFILE FOR THREE DIMENSIONAL JET.

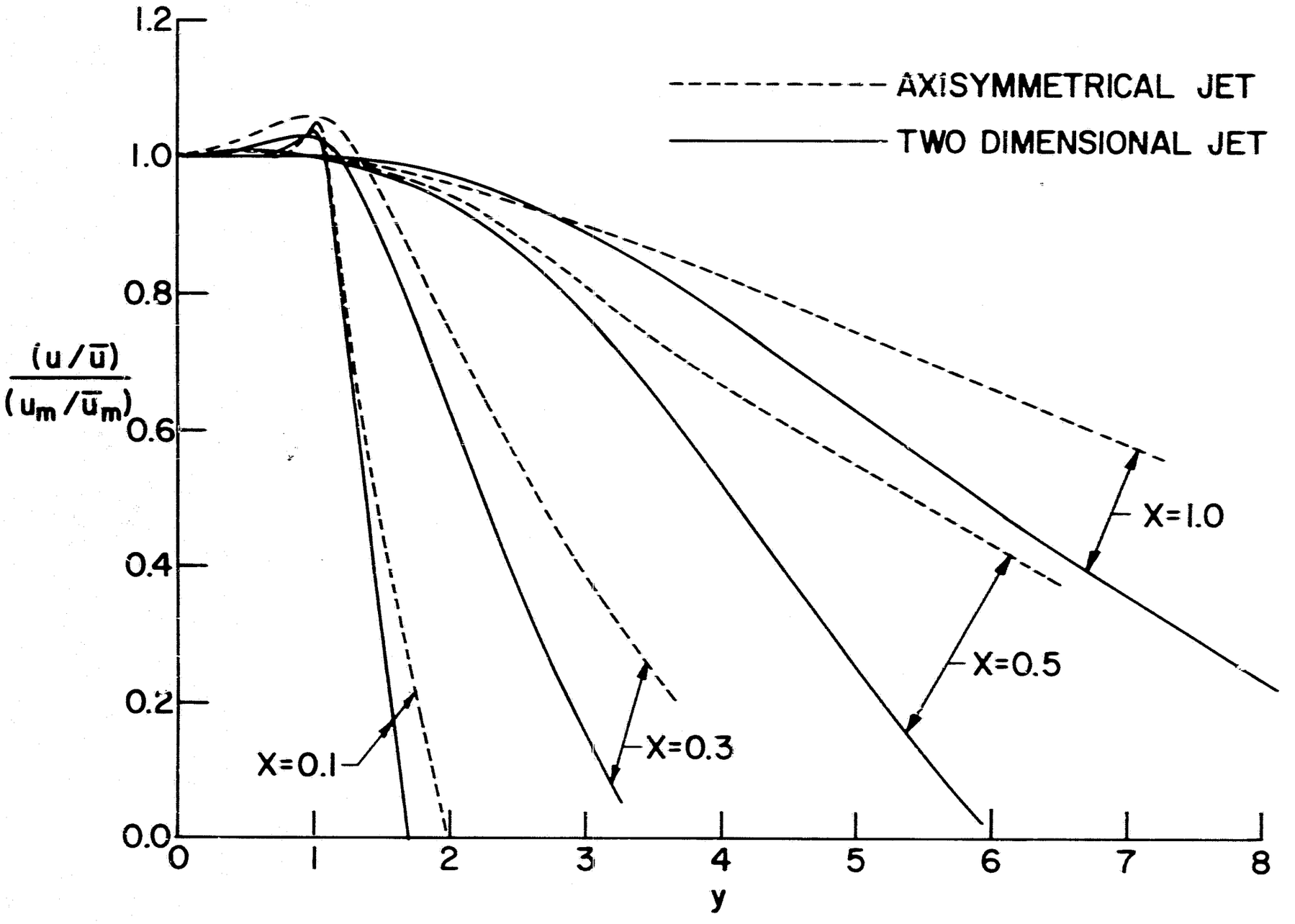

FIG. 17. $(u/\bar{u}) / (u_m/\bar{u}_m)$ vs. y

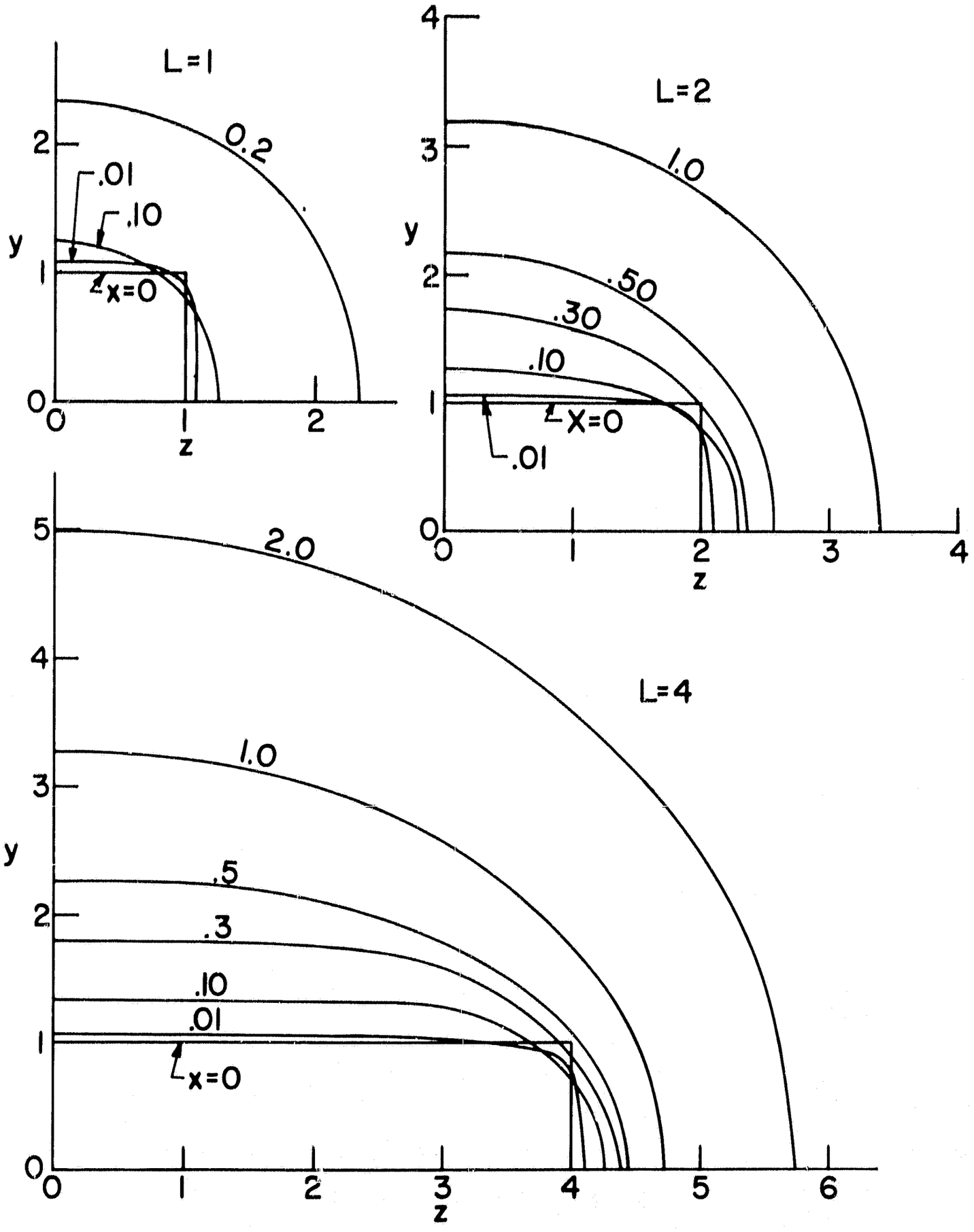

FIG. 18. CONTOUR OF HALF-WIDTH OF THREE DIMENSIONAL JET WITHOUT CROSS FLOW.